Q.2 a. Discuss the basic components of an optical communication system with block diagram. (8)

Answer:

1.3 ELEMENTS OF AN OPTICAL FIBER TRANSMISSION LINK

An optical fiber transmission link comprises the elements shown in Fig. 1-5. The key sections are a transmitter consisting of a light source and its associated drive circuitry, a cable offering mechanical and environmental protection to the optical fibers contained inside, and a receiver consisting of a photodetector plus amplification and signal-restoring circuitry. Additional components include optical amplifiers, connectors, splices, couplers, and regenerators (for restoring the signal-shape characteristics). The cabled fiber is one of the most important elements in an optical fiber link, as we shall see in Chaps. 2 and 3. In addition to protecting the glass fibers during installation and service, the cable may contain copper wires for powering optical amplifiers or signal regenerators, which are needed periodically for amplifying and reshaping the signal in long-distance links.

Analogous to copper cables, optical fiber cables can be installed either aerially, in ducts, undersea, or buried directly in the ground, as Fig. 1-6 illustrates. As a result of installation and/or manufacturing limitations, individual cable lengths will range from several hundred meters to several kilometers. Practical considerations such as reel size and cable weight determine the actual length of a single cable section. Shorter segments tend to be used when the cables are pulled through ducts. Longer lengths are used in aerial, direct-burial, or undersea applications. Splicing together individual cable sections forms continuous transmission lines for these long-distance links. For undersea installations, the splicing and repeater-installation functions are carried out on board a specially designed cable-laying ship.[18]

One of the principal characteristics of an optical fiber is its attenuation as a function of wavelength, as shown in Fig. 1-7. Early technology made exclusive use of the 800-to-900-nm wavelength band, since, in this region, the fibers made at that time exhibited a local minimum in the attenuation curve, and optical sources

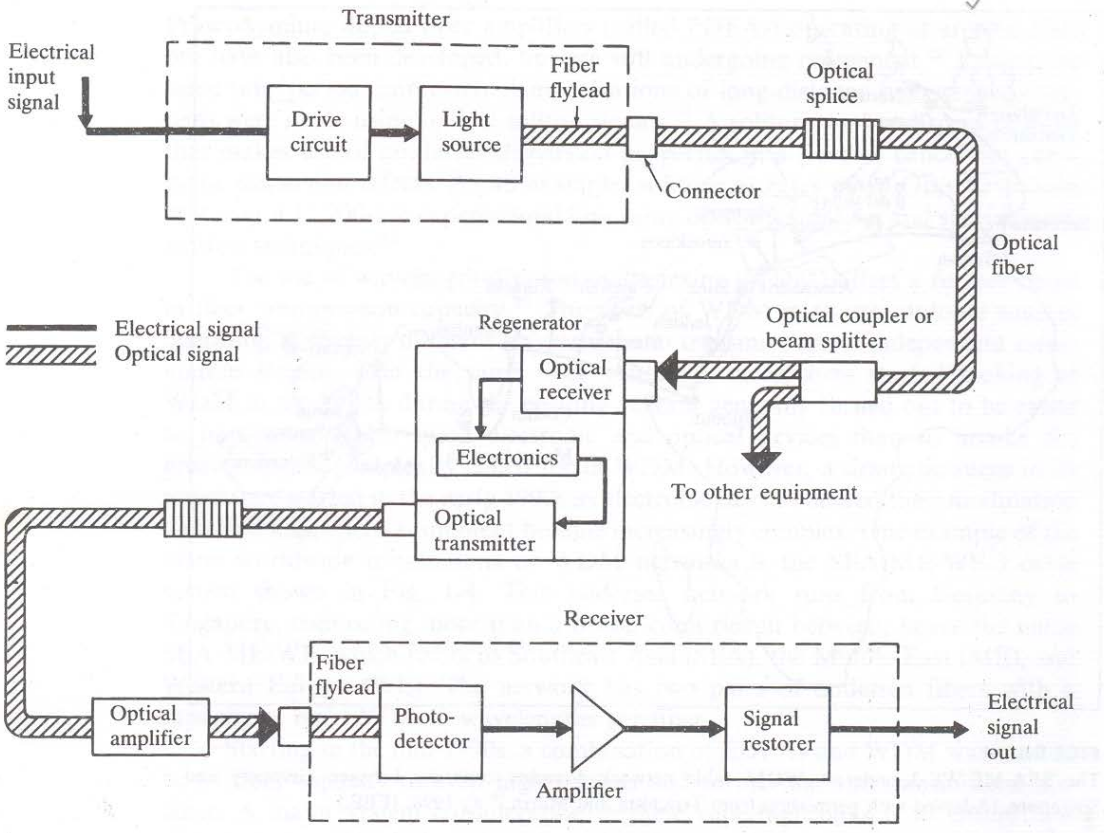

FIGURE 1-5
Major elements of an optical fiber transmission link. The basic components are the light signal transmitter, the optical fiber, and the photodetecting receiver. Additional elements include fiber and cable splices and connectors, regenerators, beam splitters, and optical amplifiers.

and photodetectors operating at these wavelengths were available. This region is referred to as the *first window*. By reducing the concentration of hydroxyl ions and metallic impurities in the fiber material, in the 1980s manufacturers were able to fabricate optical fibers with very low loss in the 1100-to-1600-nm region. This spectral band is referred to as the *long-wavelength region*. Two windows are defined here: the *second window*, centered around 1310 nm, and the *third window*, centered around 1550 nm.

In 1998 a new ultrahigh purifying process patented by Lucent Technologies eliminated virtually all water molecules from the glass fiber material. By dramatically reducing the water-attenuation peak around 1400 nm, this process opens the transmission region between the second and third windows to provide around 100 nm more bandwidth than in conventional single-mode fibers. This particular AllWave^{TM} fiber, which was specifically designed for metropolitan networks, will

give local service providers the ability to deliver cost-effectively up to hundreds of optical wavelengths simultaneously.

Once the cable is installed, a light source that is dimensionally compatible with the fiber core is used to launch optical power into the fiber. Semiconductor light-emitting diodes (LEDs) and laser diodes are suitable for this purpose, since their light output can be modulated rapidly by simply varying the bias current at the desired transmission rate, thereby producing an optical signal. The electric input signals to the transmitter circuitry for the optical source can be of either analog or digital form. For high rate systems (usually greater than 1 Gb/s), direct modulation of the source can lead to unacceptable signal distortion. In this case, an *external modulator* is used to vary the amplitude of a continuous light output from a laser diode source. In the 800-to-900-nm region the light sources are generally alloys of GaAlAs.

b. Briefly discuss the fibre classification based on modes of propagation and index profile. Draw index profile of various types of fibres. (8)

Answer:

2.3 OPTICAL FIBER MODES AND CONFIGURATIONS

Before going into details on optical fiber characteristics in Sec. 2.3.3, we first present a brief overview of the underlying concepts of optical fiber modes and optical fiber configurations.

2.3.1 Fiber Types

An optical fiber is a dielectric waveguide that operates at optical frequencies. This fiber waveguide is normally cylindrical in form. It confines electromagnetic energy in the form of light to within its surfaces and guides the light in a direction parallel to its axis. The transmission properties of an optical waveguide are dictated by its structural characteristics, which have a major effect in determining how an optical signal is affected as it propagates along the fiber. The structure basically establishes the information-carrying capacity of the fiber and also influences the response of the waveguide to environmental perturbations.

The propagation of light along a waveguide can be described in terms of a set of guided electromagnetic waves called the *modes* of the waveguide. These guided modes are referred to as the *bound* or *trapped* modes of the waveguide. Each guided mode is a pattern of electric and magnetic field distributions that is repeated along the fiber at equal intervals. Only a certain discrete number of modes are capable of propagating along the guide. As will be seen in Sec. 2.4, these modes are those electromagnetic waves that satisfy the homogeneous wave equation in the fiber and the boundary condition at the waveguide surfaces.

Although many different configurations of the optical waveguide have been discussed in the literature,[3] the most widely accepted structure is the single solid dielectric cylinder of radius a and index of refraction n_1 shown in Fig. 2-9. This cylinder is known as the *core* of the fiber. The core is surrounded by a solid dielectric *cladding* which has a refractive index n_2 that is less than n_1. Although, in principle, a cladding is not necessary for light to propagate along the core of the

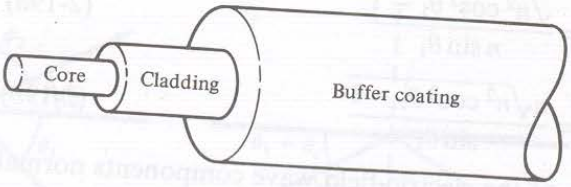

FIGURE 2-9
Schematic of a single-fiber structure. A circular solid core of refractive index n_1 is surrounded by a cladding having a refractive index $n_2 < n_1$. An elastic plastic buffer encapsulates the fiber.

fiber, it serves several purposes. The cladding reduces scattering loss that results from dielectric discontinuities at the core surface, it adds mechanical strength to the fiber, and it protects the core from absorbing surface contaminants with which it could come in contact.

In low- and medium-loss fibers the core material is generally glass and is surrounded by either a glass or a plastic cladding. Higher-loss plastic-core fibers with plastic claddings are also widely in use. In addition, most fibers are encapsulated in an elastic, abrasion-resistant plastic material. This material adds further strength to the fiber and mechanically isolates or buffers the fibers from small geometrical irregularities, distortions, or roughnesses of adjacent surfaces. These perturbations could otherwise cause scattering losses indicated by random microscopic bends that can arise when the fibers are incorporated into cables or supported by other structures.

Variations in the material composition of the core give rise to the two commonly used fiber types shown in Fig. 2-10. In the first case, the refractive index of the core is uniform throughout and undergoes an abrupt change (or step) at the cladding boundary. This is called a *step-index fiber*. In the second case, the core refractive index is made to vary as a function of the radial distance from the center of the fiber. This type is a *graded-index fiber*.

Both the step- and the graded-index fibers can be further divided into single-mode and multimode classes. As the name implies, a single-mode fiber sustains only one mode of propagation, whereas multimode fibers contain many hundreds of modes. A few typical sizes of single- and multimode fibers are given in Fig. 2-10 to provide an idea of the dimensional scale. Multimode fibers offer several advantages compared with single-mode fibers. As we shall see in Chap. 5, the larger core radii of multimode fibers make it easier to launch optical power into the fiber and facilitate the connecting together of similar fibers. Another advantage is that light can be launched into a multimode fiber using a light-emitting-diode (LED) source, whereas single-mode fibers must generally be excited with laser diodes. Although LEDs have less optical output power than laser diodes (as we shall discuss in Chap. 4), they are easier to make, are less expensive, require less complex circuitry, and have longer lifetimes than laser diodes, thus making them more desirable in certain applications.

A disadvantage of multimode fibers is that they suffer from intermodal dispersion. We shall describe this effect in detail in Chap. 3. Briefly, intermodal dispersion can be described as follows. When an optical pulse is launched into a fiber, the optical power in the pulse is distributed over all (or most) of the modes

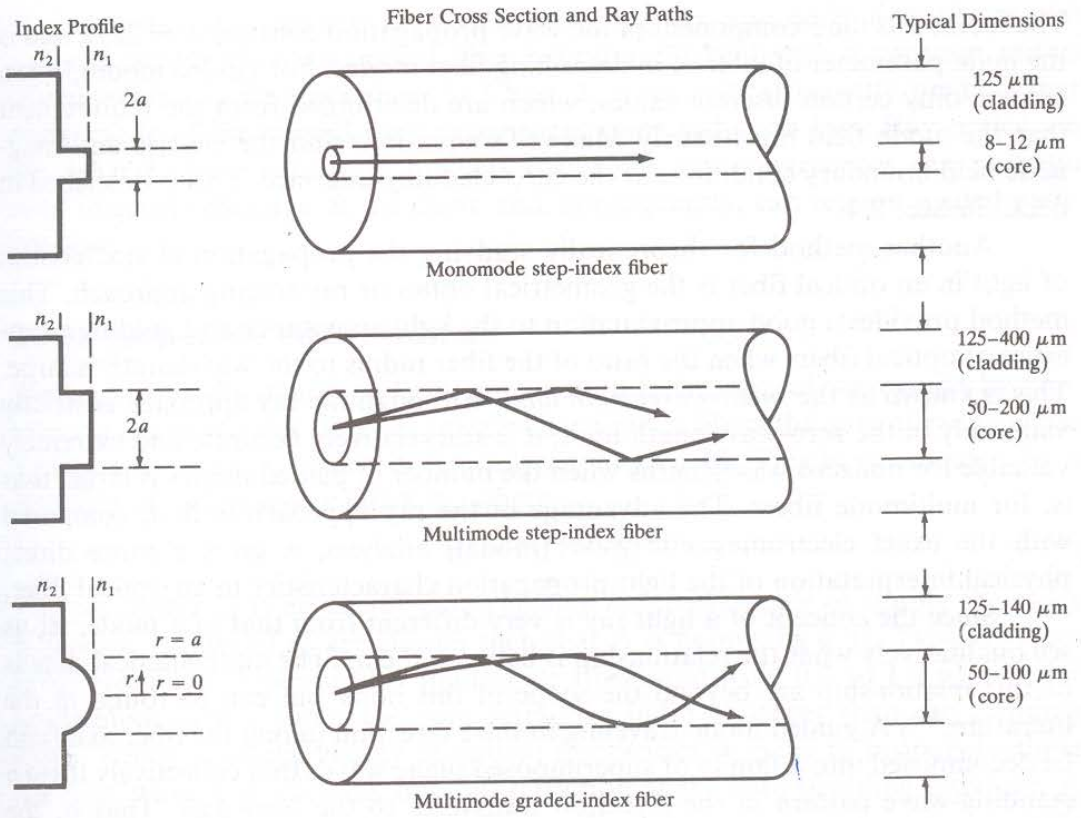

FIGURE 2-10
Comparison of single-mode and multimode step-index and graded-index optical fibers.

of the fiber. Each of the modes that can propagate in a multimode fiber travels at a slightly different velocity. This means that the modes in a given optical pulse arrive at the fiber end at slightly different times, thus causing the pulse to spread out in time as it travels along the fiber. This effect, which is known as *intermodal dispersion* or *intermodal distortion*, can be reduced by using a graded-index profile in a fiber core. This allows graded-index fibers to have much larger bandwidths (data rate transmission capabilities) then step-index fibers. Even higher bandwidths are possible in single-mode fibers, where intermodal dispersion effects are not present.

2.3.2 Rays and Modes

The electromagnetic light field that is guided along an optical fiber can be represented by a superposition of bound or trapped modes. Each of these guided modes consists of a set of simple electromagnetic field configurations. For monochromatic light fields of radian frequency ω, a mode traveling in the positive z direction (i.e., along the fiber axis) has a time and z dependence given by

$$e^{j(\omega t-\beta z)}$$

The factor β is the z component of the wave propagation constant $k = 2\pi/\lambda$ and is the main parameter of interest in describing fiber modes. For guided modes, β can assume only certain discrete values, which are determined from the requirement that the mode field must satisfy Maxwell's equations and the electric and magnetic field boundary conditions at the core–cladding interface. This is described in detail in Sec. 2.4.

Another method for theoretically studying the propagation characteristics of light in an optical fiber is the geometrical optics or ray-tracing approach. This method provides a good approximation to the light acceptance and guiding properties of optical fibers when the ratio of the fiber radius to the wavelength is large. This is known as the *small-wavelength limit*. Although the ray approach is strictly valid only in the zero-wavelength limit, it is still relatively accurate and extremely valuable for nonzero wavelengths when the number of guided modes is large; that is, for multimode fibers. The advantage of the ray approach is that, compared with the exact electromagnetic wave (modal) analysis, it gives a more direct physical interpretation of the light propagation characteristics in an optical fiber.

Since the concept of a light ray is very different from that of a mode, let us see qualitatively what the relationship is between them. (The mathematical details of this relationship are beyond the scope of this book but can be found in the literature.[4-6]) A guided mode traveling in the z direction (along the fiber axis) can be decomposed into a family of superimposed plane waves that collectively form a standing-wave pattern in the direction transverse to the fiber axis. That is, the phases of the plane waves are such that the envelope of the collective set of waves remains stationary.[2b] Since with any plane wave we can associate a light ray that is perpendicular to the phase front of the wave, the family of plane waves corresponding to a particular mode forms a set of rays called a *ray congruence*. Each ray of this particular set travels in the fiber at the same angle relative to the fiber axis. We note here that, since only a certain number M of discrete guided modes exist in a fiber, the possible angles of the ray congruences corresponding to these modes are also limited to the same number M. Although a simple ray picture appears to allow rays at any angle greater than the critical angle to propagate in a fiber, the allowable quantized propagation angles result when the phase condition for standing waves is introduced into the ray picture. This is discussed further in Sec. 2.3.5.

Despite the usefulness of the approximate geometrical optics method, a number of limitations and discrepancies exist between it and the exact modal analysis. An important case is the analysis of single-mode or few-mode fibers, which must be dealt with by using electromagnetic theory. Problems involving coherence or interference phenomena must also be solved with an electromagnetic approach. In addition, a modal analysis is necessary when a knowledge of the field distribution of individual modes is required. This arises, for example, when analyzing the excitation of an individual mode or when analyzing the coupling of power between modes at waveguide imperfections (which we shall discuss in Chap. 3).

Another discrepancy between the ray optics approach and the modal analysis occurs when an optical fiber is uniformly bent with a constant radius of curvature. As we shall show in Chap. 3, wave optics correctly predicts that every mode of the curved fiber experiences some radiation loss. Ray optics, on the other hand, erroneously predicts that some ray congruences can undergo total internal reflection at the curve and, consequently, can remain guided without loss.

2.3.3 Step-Index Fiber Structure

We begin our discussion of light propagation in an optical waveguide by considering the step-index fiber. In practical step-index fibers the core of radius a has a refractive index n_1 which is typically equal to 1.48. This is surrounded by a cladding of lightly lower index n_2, where

$$n_2 = n_1(1 - \Delta) \tag{2-20}$$

The parameter Δ is called the *core-cladding index difference* or simply the *index difference*. Values of n_2 are chosen such that Δ is nominally 0.01. Typical values range from 1 to 3 percent for multimode fibers and from 0.2 to 1.0 percent for single-mode fibers. Since the core refractive index is larger than the cladding index, electromagnetic energy at optical frequencies is made to propagate along the fiber waveguide through internal reflection at the core–cladding interface.

Q.3 a. Briefly explain the reasons for pulse broadening due to material dispersion in optical fibre. (8)

Answer:

3.2.3 Material Dispersion

Material dispersion occurs because the index of refraction varies as a function of the optical wavelength. This is exemplified in Fig. 3-12 for silica.[36] As a consequence, since the group velocity V_g of a mode is a function of the index of refraction, the various spectral components of a given mode will travel at different speeds, depending on the wavelength.[37] Material dispersion is, therefore, an intramodal dispersion effect, and is of particular importance for single-mode waveguides and for LED system (since an LED has a broader output spectrum than a laser diode).

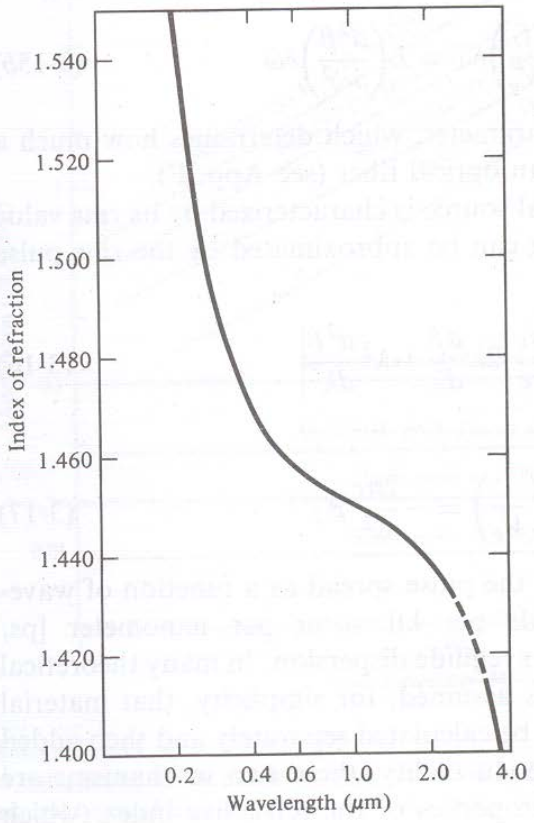

FIGURE 3-12
Variations in the index of refraction as a function of the optical wavelength for silica. (Reproduced with permission from I. H. Malitson, *J. Opt. Soc. Amer.*, vol. 55, pp. 1205–1209, Oct. 1965.)

To calculate material-induced dispersion, we consider a plane wave propagating in an infinitely extended dielectric medium that has a refractive index $n(\lambda)$ equal to that of the fiber core. The propagation constant β is thus given as

$$\beta = \frac{2\pi n(\lambda)}{\lambda} \tag{3-18}$$

Substituting this expression for β into Eq. (3-13) with $k = 2\pi/\lambda$ yields the group delay τ_{mat} resulting from material dispersion:

$$\tau_{mat} = \frac{L}{c}\left(n - \lambda\frac{dn}{d\lambda}\right) \tag{3-19}$$

Using Eq. (3-16), the pulse spread σ_{mat} for a source of spectral width σ_λ is found by differentiating this group delay with respect to wavelength and multiplying by σ_λ to yield

$$\sigma_{mat} \approx \left|\frac{d\tau_{mat}}{d\lambda}\right|\sigma_\lambda = \frac{\sigma_\lambda L}{c}\left|\lambda\frac{d^2n}{d\lambda^2}\right| = \sigma_\lambda L|D_{mat}(\lambda)| \tag{3-20}$$

where $D_{mat}(\lambda)$ is the *material dispersion*.

A plot of the material dispersion for unit length L and unit optical source spectral width σ_λ is given in Fig. 3-13 for the silica material shown in Fig. 3-12. From Eq. (3-20) and Fig. 3-13 it can be seen that material dispersion can be reduced either by choosing sources with narrower spectral output widths (reducing σ_λ) or by operating at longer wavelengths.[38]

b. A given step-index fibre has a core refractive index of 1.480, a core radius equal to 4.5 µm, and a core-cladding index difference of 0.25 percent. What is the cut off wavelength for this fibre? (8)

Answer:

{λ_c= 1230 nm} From page no. 126, numerical no. 3.14 of book OPTICAL FIBERCOMMUNICATIONS by Gred Keiser 5e publisher Mc Graw Hill Edition 2013.

Q.4 a. What are direct band-gap and indirect band-gap semiconductors? Give at least two examples of each. Which of these are suitable for fabricating LEDs and why? (8)

Answer:

4.1.4 Direct and Indirect Band Gaps

In order for electron transitions to take place to or from the conduction band with the absorption or emission of a photon, respectively, both energy and momentum must be conserved. Although a photon can have considerable energy, its momentum $h\nu/c$ is very small.

Semiconductors are classified as either *direct-band-gap* or *indirect-band-gap* materials depending on the shape of the band gap as a function of the momentum k, as shown in Fig. 4-7. Let us consider recombination of an electron and a hole, accompanied by the emission of a photon. The simplest and most probable recombination process will be that where the electron and hole have the same momentum value (see Fig. 4-7*a*). This is a direct-band-gap material.

For indirect-band-gap materials, the conduction-band minimum and the valence-band maximum energy levels occur at different values of momentum, as shown in Fig. 4-7*b*. Here, band-to-band recombination must involve a third particle to conserve momentum, since the photon momentum is very small. *Phonons* (i.e., crystal lattice vibrations) serve this purpose.

4.1.5 Semiconductor Device Fabrication

In fabricating semiconductor devices, the crystal structure of the various material regions must be carefully taken into account. In any crystal structure, single atoms (e.g., Si or Ge) or groups of atoms (e.g., NaCl or GaAs) are arranged in a repeated pattern in space. This periodic arrangement defines a *lattice*, and the

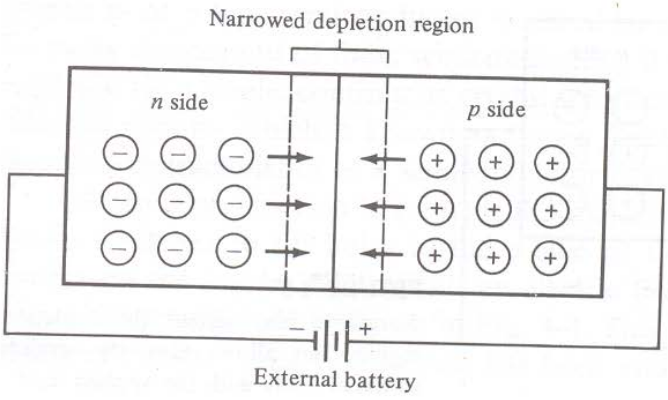

FIGURE 4-6
Lowering the barrier potential with a forward bias allows majority carriers to diffuse across the junction.

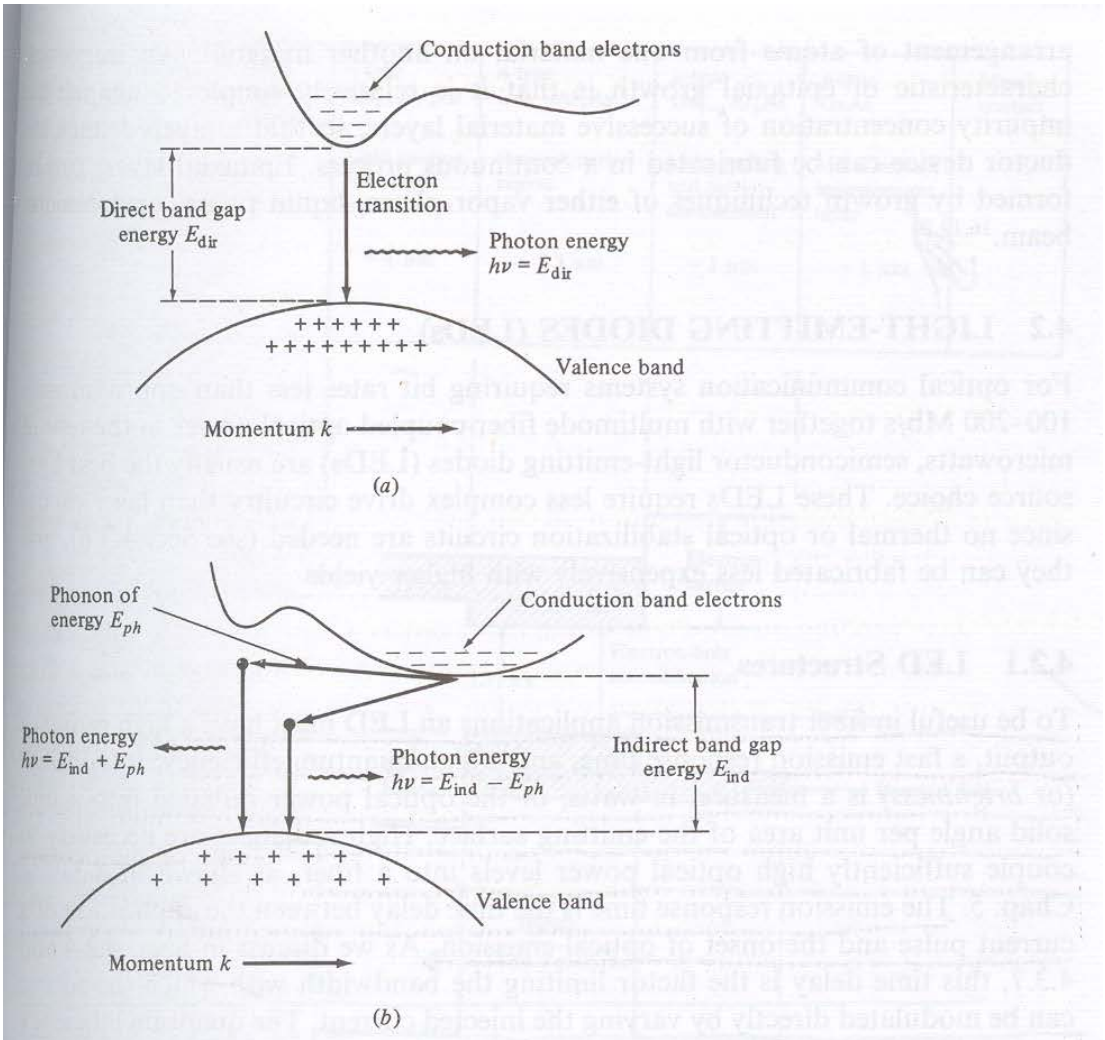

FIGURE 4-7
(*a*) Electron recombination and the associated photon emission for a direct-band-gap material; (*b*) electron recombination for indirect-band-gap materials requires a phonon of energy E_{ph} and momentum k_{ph}.

spacing between the atoms or groups of atoms is called the *lattice spacing* or the *lattice constant*. Typical lattice spacings are a few angstroms.

Semiconductor devices are generally fabricated by starting with a crystalline substrate which provides mechanical strength for mounting the device and for making electric contacts. A technique of crystal growth by chemical reaction is then used to grow thin layers of semiconductor materials on the substrate. These materials must have lattice structures that are identical to those of the substrate crystal. In particular, the lattice spacings of adjacent materials should be closely matched to avoid temperature-induced stresses and strains at the material interfaces. This type of growth is called *epitaxial*, which is derived from the Greek words *epi* meaning "on" and *taxis* meaning "arrangement"; that is, it is an

)URCES

arrangement of atoms from one material on another material. An important characteristic of epitaxial growth is that it is relatively simple to change the impurity concentration of successive material layers, so that a layered semiconductor device can be fabricated in a continuous process. Epitaxial layers can be formed by growth techniques of either vapor phase, liquid phase, or molecular beam.[16,19,20]

b. What do you meant by responsivity of photodetector? Discuss the factors responsible for limiting the speed of response of photodiode. (8)

Answer:

.2 Response Time

e response time of a photodiode together with its output circuit (see Fig. 6-8) ends mainly on the following three factors:

The transit time of the photocarriers in the depletion region.
The diffusion time of the photocarriers generated outside the depletion region.
The *RC* time constant of the photodiode and its associated circuit.

The photodiode parameters responsible for these three factors are the orption coefficient α_s, the depletion region width w, the photodiode junction package capacitances, the amplifier capacitance, the detector load resistance, amplifier input resistance, and the photodiode series resistance. The photode series resistance is generally only a few ohms and can be neglected in parison with the large load resistance and the amplifier input resistance.

Let us first look at the transit time of the photocarriers in the depletion on. The response speed of a photodiode is fundamentally limited by the time it s photogenerated carriers to travel across the depletion region. This transit t_d depends on the carrier drift velocity v_d and the depletion layer width w, is given by

$$t_d = \frac{w}{v_d} \tag{6-27}$$

eneral, the electric field in the depletion region is large enough so that the iers have reached their scattering-limited velocity. For silicon, the maximum cities for electrons and holes are 8.4×10^6 and 4.4×10^6 cm/s, respectively, n the field strength is on the order of 2×10^4 V/cm. A typical high-speed on photodiode with a 10-μm depletion layer width thus has a response time of about 0.1 ns.

The diffusion processes are slow compared with the drift of carriers in the -field region. Therefore, to have a high-speed photodiode, the photocarriers ld be generated in the depletion region or so close to it that the diffusion s are less than or equal to the carrier drift times. The effect of long diffusion s can be seen by considering the photodiode response time. This response is described by the rise time and fall time of the detector output when the tor is illuminated by a step input of optical radiation. The rise time τ_r is

typically measured from the 10- to the 90-percent points of the leading edge of the output pulse, as is shown in Fig. 6-11. For fully depleted photodiodes the rise time τ_r and fall time τ_f are generally the same. However, they can be different at low bias levels where the photodiode is not fully depleted, since the photon collection time then starts to become a significant contributor to the rise time. In this case, charge carries produced in the depletion region are separated and collected quickly. On the other hand, electron–hole pairs generated in the n and p regions must slowly diffuse to the depletion region before they can be separated and collected. A typical response time of a partially depleted photodiode is shown in Fig. 6-12. The fast carriers allow the device output to rise to 50 percent of its maximum value in approximately 1 ns, but the slow carriers cause a relatively long delay before the output reaches its maximum value.

To achieve a high quantum efficiency, the depletion layer width must be much larger than $1/\alpha_s$ (the inverse of the absorption coefficient), so that most of the light will be absorbed. The response to a rectangular input pulse of a low-capacitance photodiode having $w \gg 1/\alpha_s$ is shown in Fig. 6-13*b*. The rise and fall times of the photodiode follow the input pulse quite well. If the photodiode capacitance is larger, the response time becomes limited by the RC time constant of the load resistor R_L and the photodiode capacitance. The photodetector response then begins to appear as that shown in Fig. 6-13*c*.

If the depletion layer is too narrow, any carriers created in the undepleted material would have to diffuse back into the depletion region before they could be collected. Devices with very thin depletion regions thus tend to show distinct slow- and fast-response components, as shown in Fig. 6-13*d*. The fast component in the rise time is due to carriers generated in the depletion region, whereas the slow component arises from the diffusion of carriers that are created with a distance L_n from the edge of the depletion region. At the end of the optical pulse, the carries in

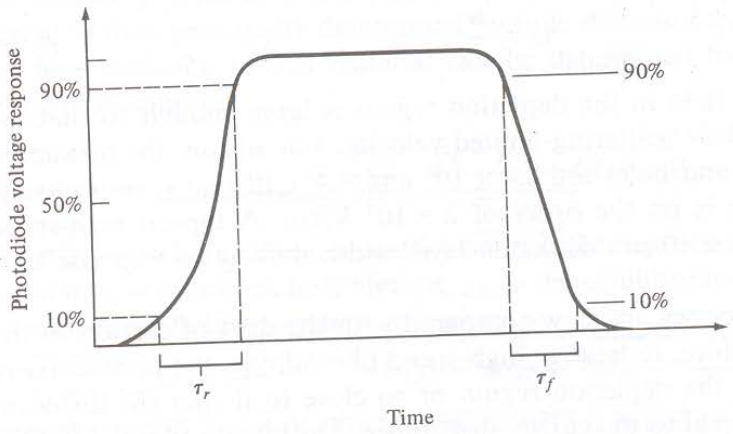

FIGURE 6-11
Photodiode response to an optical input pulse showing the 10- to 90-percent rise time and the 10- to 90-percent fall time.

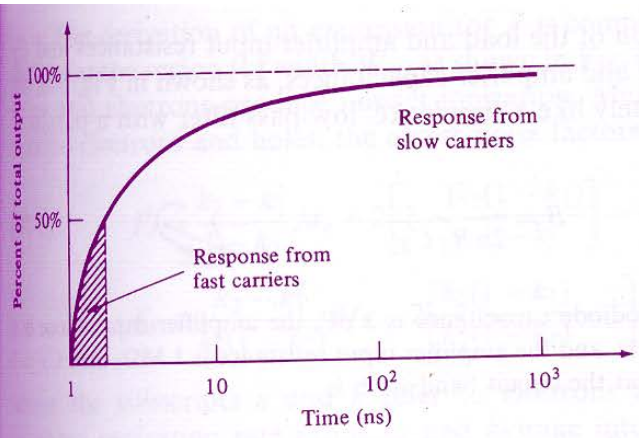

FIGURE 6-12
Typical response time of a photodiode that is not fully depleted.

the depletion region are collected quickly, which results in the fast-detector-response component in the fall time. The diffusion of carriers which are within a distance L_n of the depletion region edge appears as the slowly decaying tail at the end of the pulse. Also, if w is too thin, the junction capacitance will become excessive. The junction capacitance C_j is

$$C_j = \frac{\epsilon_s A}{w} \tag{6-28}$$

where ϵ_s = the permittivity of the semiconductor material $= \epsilon_0 K_s$
K_s = the semiconductor dielectric constant
ϵ_0 = 8.8542×10^{-12} F/m is the free-space permittivity
A = the diffusion layer area

This excessiveness will then give rise to a large RC time constant which limits the detector response time. A reasonable compromise between high-frequency response and high quantum efficiency is found for absorption region thicknesses between $1/\alpha_s$ and $2/\alpha_s$.

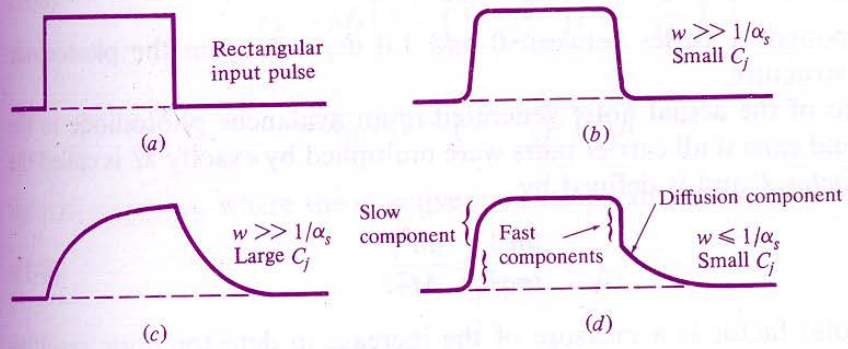

FIGURE 6-13
Photodiode pulse responses under various detector parameters.

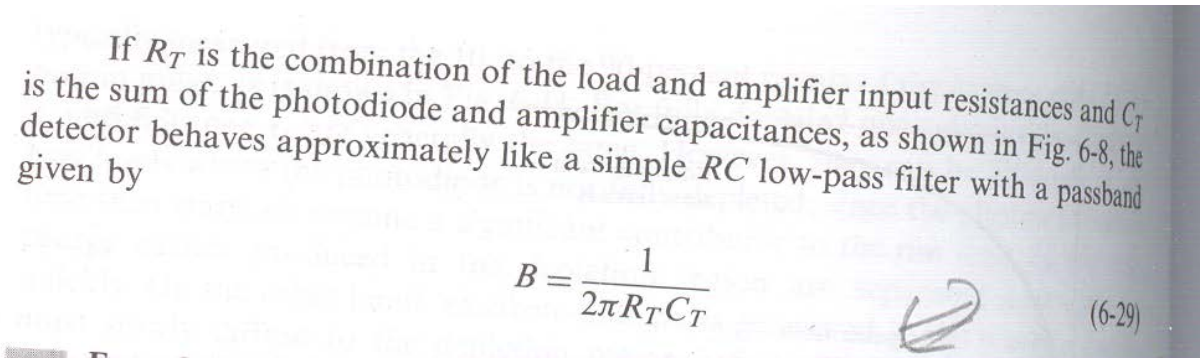

If R_T is the combination of the load and amplifier input resistances and C_T is the sum of the photodiode and amplifier capacitances, as shown in Fig. 6-8, the detector behaves approximately like a simple RC low-pass filter with a passband given by

$$B = \frac{1}{2\pi R_T C_T} \qquad (6\text{-}29)$$

Q.5 a. Discuss various lensing schemes used for the improvement of coupling of light to the fibre and outline the technique deployed for the LED coupling to Single Mode Fibre. (8)

Answer:

5.2 LENSING SCHEMES FOR COUPLING IMPROVEMENT

The optical power-launching analysis given in Sec. 5.1 is based on centering a fiber end face directly over the light source as close to it as possible. If the sou emitting area is larger than the fiber-core area, then the resulting optical pow coupled into the fiber is the maximum that can be achieved. This is a result fundamental energy and radiance conservation principles[6] (also known as the *of brightness*). However, if the emitting area of the source is smaller than the co area, a miniature lens may be placed between the source and the fiber to impro the power-coupling efficiency.

The function of the microlens is to magnify the emitting area of the sour to match exactly the core area of the fiber end face. If the emitting area increased by a magnification factor M, the solid angle within which optica power is coupled to the fiber from the LED is increased by the same factor.

Several possible lensing schemes[1,7-12] are shown in Fig. 5-5. These include rounded-end fiber, a small glass sphere (nonimaging microsphere) in contact with both the fiber and the source, a larger spherical lens used to image the source or the core area of the fiber end, a cylindrical lens generally formed from a short section of fiber, a system consisting of a spherical-surfaced LED and a spherical-ended fiber, and a taper-ended fiber.

Although these techniques can improve the source-to-fiber coupling efficiency, they also create additional complexities. One problem is that the lens size is similar to the source and fiber-core dimensions, which introduces fabrication and handling difficulties. In the case of the taper-ended fiber, the mechanical alignment must be carried out with greater precision since the coupling efficiency

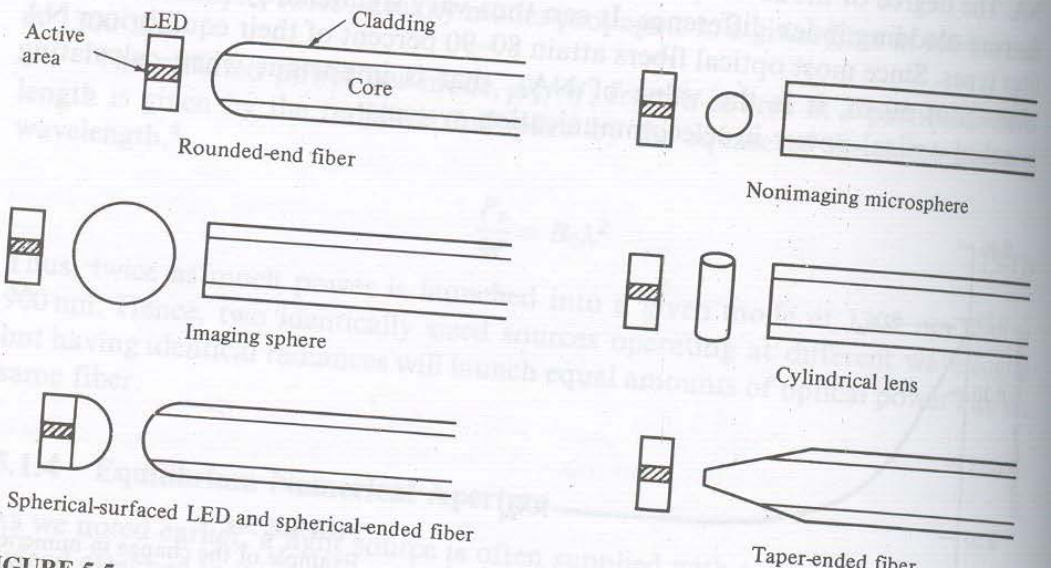

FIGURE 5-5
Examples of possible lensing schemes used to improve optical source-to-fiber coupling efficiency.

5.2.1 Nonimaging Microsphere

One of the most efficient lensing methods is the use of a nonimaging microsphere. Let us first examine its use for a surface emitter, as shown in Fig. 5-6. We first make the following practical assumptions: the spherical lens has a refractive index of about 2.0, the outside medium is air ($n = 1.0$), and the emitting area is circular. To collimate the output from the LED, the emitting surface should be located at the focal point of the lens. The focal point can be found from the gaussian lens formula[13]

$$\frac{n}{s} + \frac{n'}{q} = \frac{n' - n}{r} \tag{5-14}$$

where s and q are the object and image distances, respectively, as measured from the lens surface, n is the refractive index of the lens, n' is the refractive index of the outside medium, and r is the radius of curvature of the lens surface.

The following sign conventions are used with Eq. (5-14):

1. Light travels from left to right.
2. Object distances are measured as positive to the left of a vertex and negative to the right.
3. Image distances are measured as positive to the right of a vertex and negative to the left.
4. All convex surfaces encountered by the light have a positive radius of curvature, and concave surfaces have a negative radius.

With the use of these conventions, we shall now find the focal point for the right-hand surface of the lens shown in Fig. 5-6. To find the focal point, we set $q = \infty$ and solve for s in Eq. (5-14), where s is measured from point B. With $n = 2.0$, $n' = 1.0$, $q = \infty$, and $r = -R_L$, Eq. (5-14) yields

$$s = f = 2R_L$$

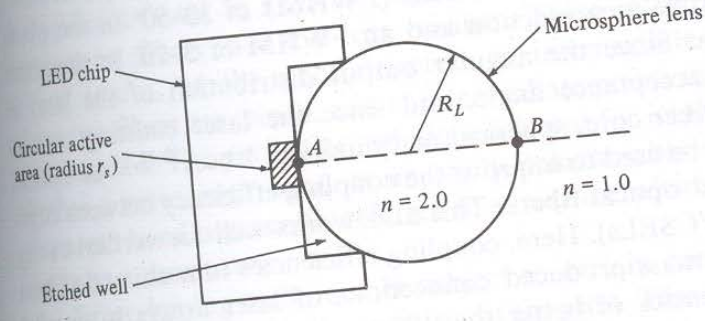

FIGURE 5-6
Schematic diagram of an LED emitter with a microsphere lens.

Thus, the focal point is located on the lens surface at point A. (This, of course, changes if the refractive index of the sphere is not equal to 2.0.)

Placing the LED close to the lens surface thus results in a magnification M of the emitting area. This is given by the ratio of the cross-sectional area of the lens to that of the emitting area:

$$M = \frac{\pi R_L^2}{\pi r_s^2} = \left(\frac{R_L}{r_s}\right)^2 \tag{5-15}$$

Using Eq. (5-4) we can show that, with the lens, the optical power P_L that can be coupled into a full aperture angle 2θ is given by

$$P_L = P_s\left(\frac{R_L}{r_s}\right)^2 \sin^2\theta \tag{5-16}$$

where P_s is the total output power from the LED without the lens.

The theoretical coupling efficiency that can be achieved is based on energy and radiance conservation principles.[14] This efficiency is usually determined by the size of the fiber. For a fiber of radius a and numerical aperture NA, the maximum coupling efficiency $\eta_{\max}$ is given by

$$\eta_{\max} = \begin{cases} \left(\frac{a}{r_s}\right)^2 (\text{NA})^2 & \text{for} \quad \frac{r_s}{a} > \text{NA} \\ 1 & \text{for} \quad \frac{r_s}{a} \le \text{NA} \end{cases} \tag{5-17}$$

Thus, when the radius of the emitting area is larger than the fiber radius, no improvement in coupling efficiency is possible with a lens. In this case, the best coupling efficiency is achieved by a direct-butt method.

Based on Eq. (5-17), the theoretical coupling efficiency as a function of the emitting diameter is shown in Fig. 5-7 for a fiber with a numerical aperture of 0.20 and 50-μm core diameter.

b. What do you understand by optical fibre connectors? List all the necessary requirements of a good connector. Also, discuss the popular alignment schemes used in optic connectors. (8)

Answer:

5.6 OPTICAL FIBER CONNECTORS

A wide variety of optical fiber connectors has evolved for numerous different applications. Their uses range from simple single-channel fiber-to-fiber connectors in a benign location to multichannel connectors used in harsh military field environments. Some of the principal requirements of a good connector design are as follows:

1. *Low coupling losses*. The connector assembly must maintain stringent alignment tolerances to assure low mating losses. These low losses must not change significantly during operation or after numerous connects and disconnects.
2. *Interchangeability*. Connectors of the same type must be compatible from one manufacturer to another.
3. *Ease of assembly*. A service technician should readily be able to install the connector in a field environment; that is, in a location other than the connector factory. The connector loss should also be fairly insensitive to the assembly skill of the technician.
4. *Low environmental sensitivity*. Conditions such as temperature, dust, and moisture should have a small effect on connector-loss variations.
5. *Low-cost and reliable construction*. The connector must have a precision suitable to the application, but its cost must not be a major factor in the fiber system.
6. *Ease of connection*. Generally, one should be able to mate and demate the connector, simply, by hand.

5.6.1 Connector Types

Connectors are available in screw-on, bayonet-mount, and push–pull configurations.[55,63-74] These include both single-channel and multichannel assemblies for cable-to-cable and for cable-to-circuit card connections. The basic coupling mechanisms used in these connectors belong to either the *butt-joint* or the *expanded-beam* classes.

Butt-joint connectors employ a metal, ceramic, or molded-plastic ferrule for each fiber and a precision sleeve into which the ferrule fit. The fiber is epoxied into a precision hole which has been drilled into the ferrule. The mechanical challenges of ferrule connectors include maintaining both the dimensions of the hole diameter and its position relative to the ferrule outer surface.

Figure 5-20 shows two popular butt-joint alignment designs used in both multimode and single-mode fiber systems. These are the *straight-sleeve* and the *tapered-sleeve* (or *biconical*) mechanisms. In the straight-sleeve connector, the length of the sleeve and a guide ring on the ferrules determine the end separation of the fibers. The biconical connector uses a tapered sleeve to accept and guide tapered ferrules. Again, the sleeve length and the guide rings maintain a given fiber-end separation.

An expanded-beam connector, illustrated in Fig. 5-21, employs lenses on the ends of the fibers. These lenses either collimate the light emerging from the transmitting fiber, or focus the expanded beam onto the core of the receiving fiber. The fiber-to-lens distance is equal to the focal length of the lens. The advantage of this scheme is that, since the beam is collimated, separation of the fiber ends may take place within the connector. Thus, the connector is less dependent on lateral alignments. In addition, optical processing elements, such as beam splitters and switches, can easily be inserted into the expanded beam between the fiber ends.

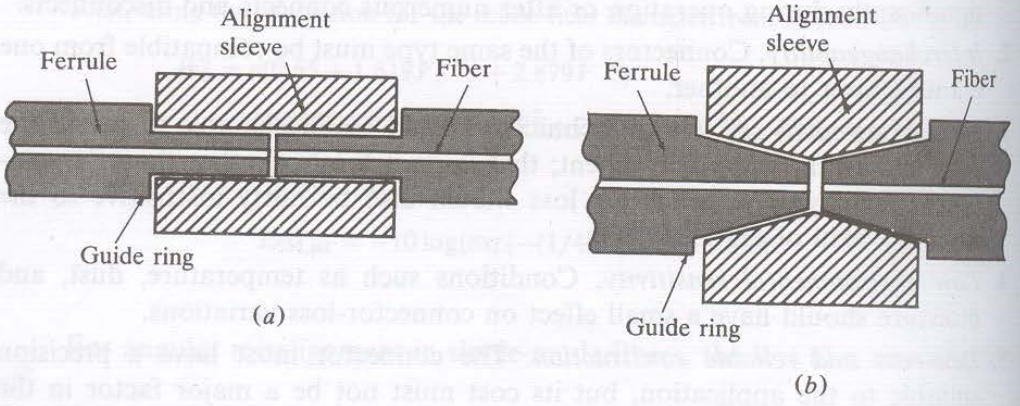

FIGURE 5-20
Examples of two popular alignment schemes used in fiber optic connectors: (*a*) straight sleeve, (*b*) tapered sleeve.

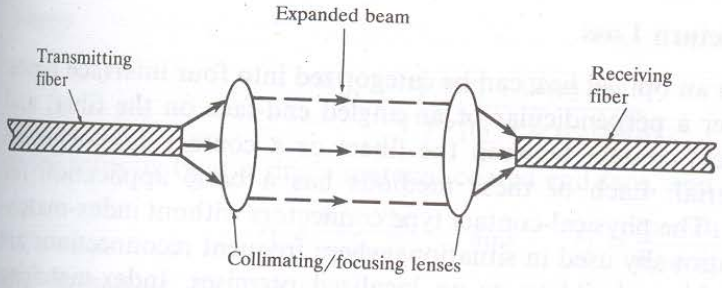

FIGURE 5-21
Schematic representation of an expanded-beam fiber optic connector.

5.6.2 Single-Mode Fiber Connectors

Because of the wide use of single-mode fiber optic links and because of the greater alignment precision required for these systems, this section addresses single-mode connector coupling losses. Based on the gaussian-beam model of single-mode fiber fields,[63] Nemota and Makimoto[75] derived the following coupling loss (in decibels) between single-mode fibers that have unequal mode-field diameters (which is an intrinsic factor) and lateral, longitudinal, and angular offsets plus reflections (which are all extrinsic factors):

$$L_{SM;ff} = -10\log\left[\frac{16n_1^2n_3^2}{(n_1+n_3)^4}\frac{4\sigma}{q}\exp\left(-\frac{\rho u}{q}\right)\right] \tag{5-43}$$

where $\rho = (kW_1)^2$

$q = G^2 + (\sigma+1)^2$

$u = (\sigma+1)F^2 + 2\sigma FG\sin\theta + \sigma(G^2+\sigma+1)\sin^2\theta$

$F = \dfrac{d}{kW_1^2}$

$G = \dfrac{s}{kW_1^2}$

$\sigma = (W_2/W_1)^2$

$k = 2\pi n_3/\lambda$

n_1 = core refractive index of fibers

n_3 = refractive index of medium between fibers

λ = wavelength of source

d = lateral offset

s = longitudinal offset

θ = angular misalignment

W_1 = $1/e$ mode-field radius of transmitting fiber

W_2 = $1/e$ mode-field radius of receiving fiber

This general equation gives very good correlation with experimental investigations.[64]

5.6.3 Connector Return Loss

A connection point in an optical link can be categorized into four interface types. These consist of either a perpendicular or an angled end-face on the fiber, and either a direct physical contact between the fibers or a contact employing an index-matching material. Each of these methods has a basic application for which it is best suited. The physical-contact type connectors without index-matching material are traditionally used in situations where frequent reconnections are required, such as within a building or on localized premises. Index-matching connectors are standardly employed in outside cable plants where the reconnections are infrequent, but need to have a low loss.

This section gives some details on index-matched and direct physical contacts, and briefly discusses angled interfaces. In each case, these connections require high return losses (low reflection levels) and low insertion loses (high optical-signal throughput levels). The low reflectance levels are desired since optical reflections provide a source of unwanted feedback into the laser cavity. This can affect the optical frequency response, the linewidth, and the internal noise of the laser, which results in degradation of system performance.

Figure 5-22 shows a model of an index-matched connection with perpendicular fiber end faces. In this figure and in the following analyses, offsets and angular misalignments are not taken into account. The connection model shows that the fiber end faces have a thin surface layer of thickness h having a high refractive index n_2 relative to the core index, which is a result of fiber polishing. The fiber core has an index n_0, and the gap width d between the end faces is filled with index-matching material having a refractive index n_1. The return loss RL_{IM} in decibels for the index-matched gap region is given by[76]

$$RL_{IM} = -10\log\left\{2R\left[1-\cos\left(\frac{4\pi n_1 d}{\lambda}\right)\right]\right\} \tag{5-44}$$

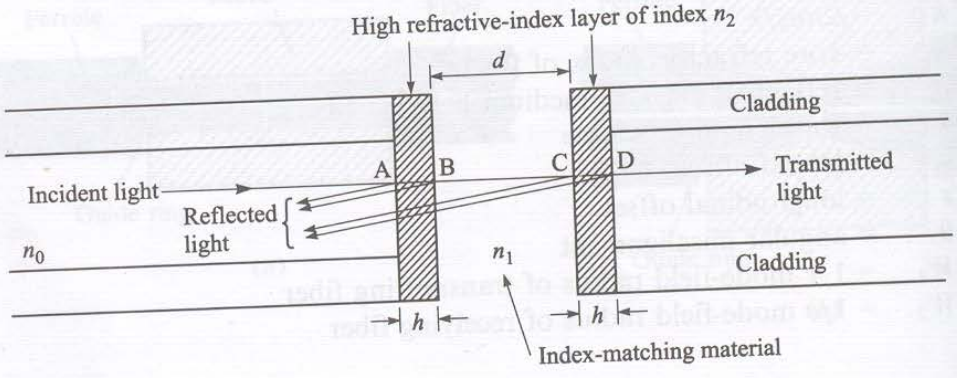

FIGURE 5-22
Model of an index-matched connection with perpendicular fiber end faces.

where

$$R = \frac{r_1^2 + r_2^2 + 2r_1 r_2 \cos\delta}{1 + r_1^2 r_2^2 + 2r_1 r_2 \cos\delta} \tag{5-45}$$

is the reflectivity at a single material-coated end face, and

$$r_1 = \frac{n_0 - n_2}{n_0 + n_2} \quad \text{and} \quad r_2 = \frac{n_2 - n_1}{n_2 + n_1} \tag{5-46}$$

are the reflection coefficients through the core from the high-index layer and through the high-index layer from the core, respectively. The parameter $\delta = (4\pi/\lambda)n_2 h$ is the phase difference in the high-index layer. The factor 2 in Eq. (5-44) accounts for reflections at both fiber end faces. The value of n_2 of the glass surface layer varies from 1.46 to 1.60, and the thickness h ranges from 0 to 0.15 μm.

When the perpendicular end faces are in direct physical contact, the return loss RL_{PC} in decibels is given by[76]

$$\mathrm{RL}_{PC} = -10\log\left\{2R_2\left[1 - \cos\left(\frac{4\pi n_2}{\lambda}2h\right)\right]\right\} \tag{5-47}$$

where

$$R_2 = \left(\frac{n_0 - n_2}{n_0 + n_2}\right)^2 \tag{5-48}$$

Here, R_2 is the reflectivity at the discontinuity between the refractive indices of the fiber core and the high-index surface layer. In this case, the return loss at a given wavelength depends on the value of the refractive index n_2 and the thickness h of the surface layer.

Connections with angled end-faces are used in applications where an ultra-low reflection is required. Figure 5-23 shows a cross-sectional view of such a connection with a small gap of width d separating the fiber ends. The fiber

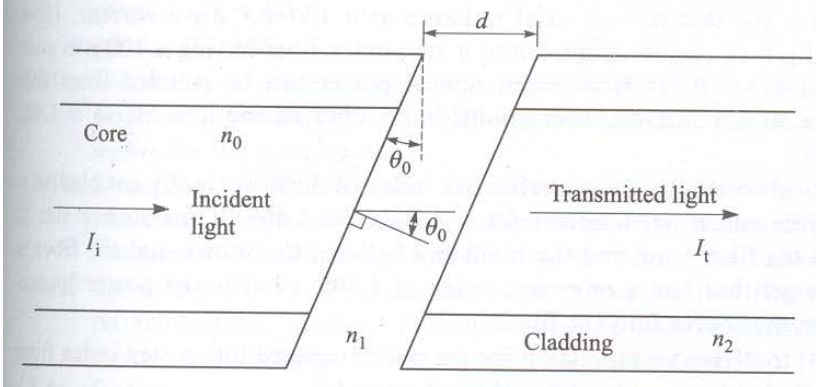

FIGURE 5-23
Connection with angled end faces having a small gap of width d separating the fiber ends.

core has an index n_0, and the material in the gap has a refractive index n_1. The end faces are polished at an angle θ_0 with respect to the plane perpendicular to the fiber axis. This angle is typically 8°. If I_i and I_t are the incident and throughput optical power intensities, respectively, then the transmitted efficiency T through the connector is[77]

$$T = \frac{I_t}{I_i} = \frac{(1-R)^2}{(1-R)^2 + 4R\sin^2(\beta/2)} \tag{5-49}$$

where

$$\frac{\sin\theta_0}{\sin\theta} = \frac{n}{n_0}, \qquad \beta = \frac{4\pi n_1 d\cos\theta}{\lambda}, \qquad \text{and} \qquad R = \left(\frac{n_0 - n_1}{n_0 + n_1}\right)^2$$

The insertion loss for this type of connector with an 8° angle will vary from 0 dB for no gap to 0.6 dB for an air gap of width $d = 1.0\,\mu$m. Note that when an index-matching material is used so that $n_0 = n_1$, then $R = 0$ and $T = 1$. When $n_0 \neq n_1$, the transmitted efficiency (and hence the connector loss) has an oscillatory behavior as a function of the wavelength and the end-face angle.

Q.6 a. Derive an error probability expression for a digital receiver. (8)

Answer:

7.2.1 Probability of Error

In practice, there are several standard ways of measuring the rate of error occurrences in a digital data stream.[22] One common approach is to divide the number N_e of errors occuring over a certain time interval t by the number N_t of pulses (ones and zeros) transmitted during this interval. This is called either the *error rate* or the *bit-error rate*, which is commonly abbreviated BER. Thus, we have

$$\text{BER} = \frac{N_e}{N_t} = \frac{N_e}{Bt} \tag{7-15}$$

where $B = 1/T_b$ is the bit rate (i.e., the pulse transmission rate). The error rate is expressed by a number, such as 10^{-9}, for example, which states that, on the average, one error occurs for every billion pulses sent. Typical error rates for optical fiber telecommunication systems range from 10^{-9} to 10^{-12}. This error rate depends on the signal-to-noise ratio at the receiver (the ratio of signal power to noise power). The system error rate requirements and the receiver noise levels thus set a lower limit on the optical signal power level that is required at the photodetector.

To compute the bit-error rate at the receiver, we have to know the probability distribution[23] of the signal at the equalizer output. Knowing the signal probability distribution at this point is important because it is here that the decision is made as to whether a 0 or a 1 is sent. The shapes of two signal probability distributions are shown in Fig. 7-5. These are

$$P_1(v) = \int_{-\infty}^{v} p(y|1)\, dy \tag{7-16}$$

which is the probability that the equalizer output voltage is less than v when a logical 1 pulse is sent, and

$$P_0(v) = \int_{v}^{\infty} p(y|0)\, dy \tag{7-17}$$

which is the probability that the output voltage exceeds v when a logical 0 is transmitted. Note that the different shapes of the two probability distributions in Fig. 7-5 indicate that the noise power for a logical 0 is usually not the same as that for a logical 1. This occurs in optical systems because of signal distortion from transmission impairments (e.g., dispersion, optical amplifier noise, and distortion from nonlinear effects) and from noise and ISI contributions at the receiver. The functions $p(y|1)$ and $p(y|0)$ are the conditional probability distribu-

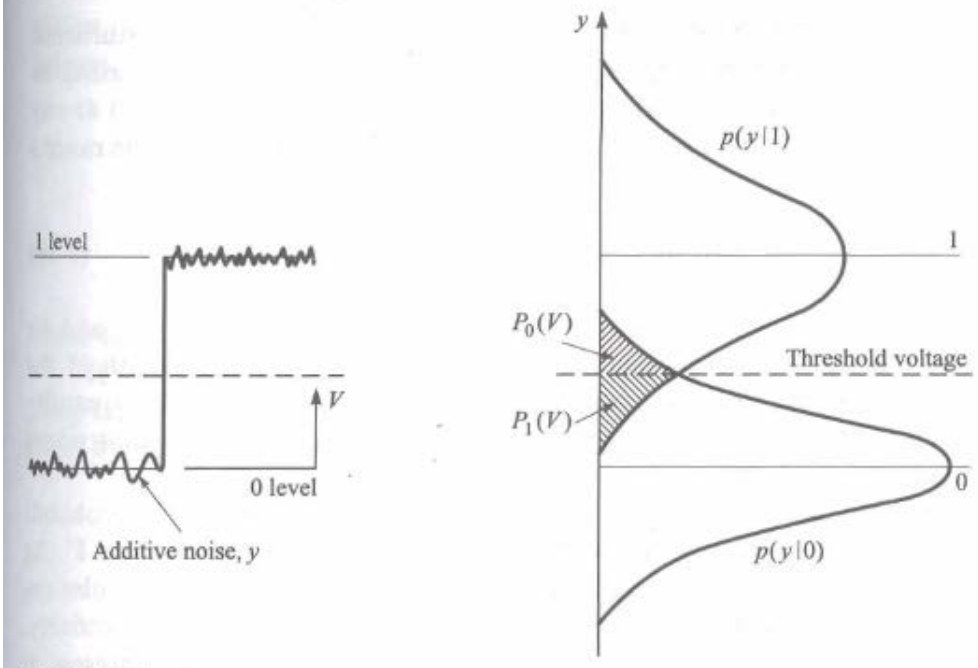

FIGURE 7-5
Probability distributions for received logical 0 and 1 signal pulses. The different widths of the two distributions are caused by various signal distortion effects.

tion functions;[9,23] that is, $p(y|x)$ is the probability that the output voltage is y, given that an x was transmitted.

If the threshold voltage is v_{th} then the error probability P_e is defined as

$$P_e = aP_1(v_{th}) + bP_0(v_{th}) \tag{7-18}$$

The weighting factors a and b are determined by the a priori distribution of the data. That is, a and b are the probabilities that either a 1 or a 0 occurs, respectively. For unbiased data with equal probability of 1 and 0 occurrences, $a = b = 0.5$. The problem to be solved now is to select the decision threshold at that point where P_e is minimum.

To calculate the error probability we require a knowledge of the mean-square noise voltage $\langle v_N^2 \rangle$ which is superimposed on the signal voltage at the decision time. The statistics of the output voltage at the sampling time are very complicated, so that an exact calculation is rather tedious to perform. A number of different approximations[1–18] have therefore been used to calculate the performance of a binary optical fiber receiver. In applying these approximations, we have to make a tradeoff between computational simplicity and accuracy of the results. The simplest method is based on a gaussian approximation. In this method, it is assumed that, when the sequence of optical input pulses is known, the equalizer output voltage $v_{out(t)}$ is a gaussian random variable. Thus, to calculate the error probability, we need only to know the mean and standard deviation of $v_{out}(t)$. Other approximations that have been investigated are more involved[4–6,16–18] and will not be discussed here.

Thus, let us assume that a signal s (which can be either a noise disturbance or a desired information-bearing signal) has a gaussian probability distribution function with a mean value m. If we sample the signal voltage level $s(t)$ at any arbitrary time t_1, the probability that the measured sample $s(t_1)$ falls in the range s to $s + ds$ is given by

$$f(s)\,ds = \frac{1}{\sqrt{2\pi\sigma^2}} e^{-(s-m)^2/2\sigma^2} ds \tag{7-19}$$

where $f(s)$ is the *probability density function*, σ^2 is the noise variance, and its square root σ is the *standard deviation*, which is a measure of the width of the probability distribution. By examining Eq. (7-19) we can see that the quantity $2\sqrt{2}\sigma$ measures the full width of the probability distribution at the point where the amplitude is $1/e$ of the maximum.

We can now use the probability density function to determine the probability of error for a data stream in which the 1 pulses are all of amplitude V. As shown in Fig. 7-6, the mean and variance of the gaussian output for a 1 pulse are b_{on} and σ_{on}^2, respectively, whereas for a 0 pulse they are b_{off} and σ_{off}^2, respectively. Let us first consider the case of a 0 pulse being sent, so that no pulse is present at the decoding time. The probability of error in this case is the probability that the noise will exceed the threshold voltage v_{th} and be mistaken for a 1 pulse. This probability of error $P_0(v)$ is the chance that the equalizer output voltage $v(t)$ will fall somewhere between v_{th} and ∞. Using Eqs. (7-17) and (7-19), we have

$$\begin{aligned} P_0(v_{th}) &= \int_{v_{th}}^{\infty} p(y|0)dy = \int_{v_{th}}^{\infty} f_0(y)dy \\ &= \frac{1}{\sqrt{2\pi}\sigma_{off}} \int_{v_{th}}^{\infty} \exp\left[-\frac{(v - b_{off})^2}{2\sigma_{off}^2}\right] dv \end{aligned} \tag{7-20}$$

where the subscript 0 denotes the presence of a 0 bit.

Similarly, we can find the probability of error that a transmitted 1 is misinterpreted as a 0 by the decoder electronics following the equalizer. This prob-

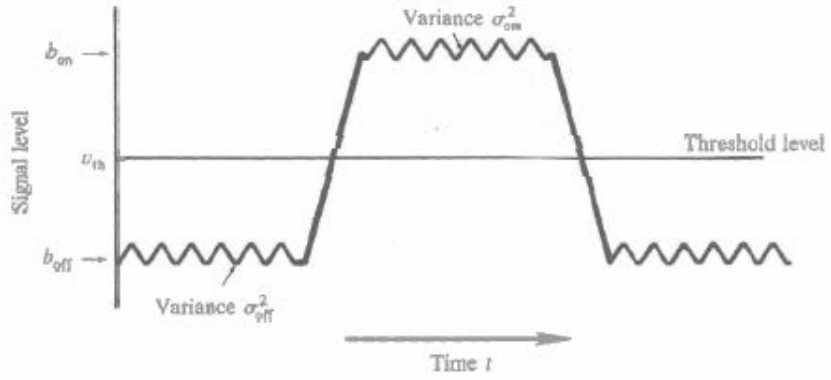

FIGURE 7-6
Gaussian noise statistics of a binary signal showing variances about the on and off signal levels.

ability of error is the likelihood that the sampled signal-plus-noise pulse falls below v_{th}. From Eqs. (7-16) and (7-19), this is simply given by

$$P_1(v_{th}) = \int_{-\infty}^{v_{th}} p(y|1)dy = \int_{-\infty}^{v_{th}} f_1(v)dv$$
$$= \frac{1}{\sqrt{2\pi}\sigma_{on}} \int_{-\infty}^{v_{th}} \exp\left[-\frac{(b_{on} - v)^2}{2\sigma_{on}^2}\right] dv \quad (7\text{-}21)$$

where the subscript 1 denotes the presence of a 1 bit.

If we assume that the probabilities of 0 and 1 pulses are equally likely, then, using Eqs. (7-20) and (7-21), the bit-error rate (BER) or the error probability P_e given by Eq. (7-18) becomes

$$\text{BER} = P_e(Q) = \frac{1}{\sqrt{\pi}} \int_{Q/\sqrt{2}}^{\infty} e^{-x^2} dx$$
$$= \frac{1}{2}\left[1 - \text{erf}\left(\frac{Q}{\sqrt{2}}\right)\right] \approx \frac{1}{\sqrt{2\pi}} \frac{e^{-Q^2/2}}{Q} \quad (7\text{-}22)$$

The approximation is obtained from the asymptotic expansion of erf(x). Here, the parameter Q is defined as

$$Q = \frac{v_{th} - b_{off}}{\sigma_{off}} = \frac{b_{on} - v_{th}}{\sigma_{on}} \quad (7\text{-}23)$$

and

$$\text{erf}(x) = \frac{2}{\sqrt{\pi}} \int_0^x e^{-y^2} dy \quad (7\text{-}24)$$

is the *error function*, which is tabulated in various mathematical handbooks.[24]

The factor Q is widely used to specify receiver performance, since it is related to the signal-to-noise ratio required to achieve a specific bit-error rate.[25] In particular, it takes into account that in optical fiber systems the variances in the noise powers generally are different for received logical 0 and 1 pulses. Figure 7-7 shows how the BER varies with Q. The approximation for P_e given in Eq. (7-22) and shown by the dashed line in Fig. 7-7 is accurate to 1 percent for $Q \approx 3$ and improves as Q increases. A commonly quoted Q value is 6, since this corresponds to a BER $= 10^{-9}$.

Let us consider the special case when $\sigma_{off} = \sigma_{on} = \sigma$ and $b_{off} = 0$, so that $b_{on} = V$. Then, from Eq. (7-23) we have that the threshold voltage $v_{th} = V/2$, so that $Q = V/2\sigma$. Since σ is usually called the *rms noise*, the ratio V/σ is the *peak signal-to-rms-noise ratio*. In this case, Eq. (7-22) becomes

$$P_e(\sigma_{on} = \sigma_{off}) = \frac{1}{2}\left[1 - \text{erf}\left(\frac{V}{2\sqrt{2}\sigma}\right)\right] \quad (7\text{-}25)$$

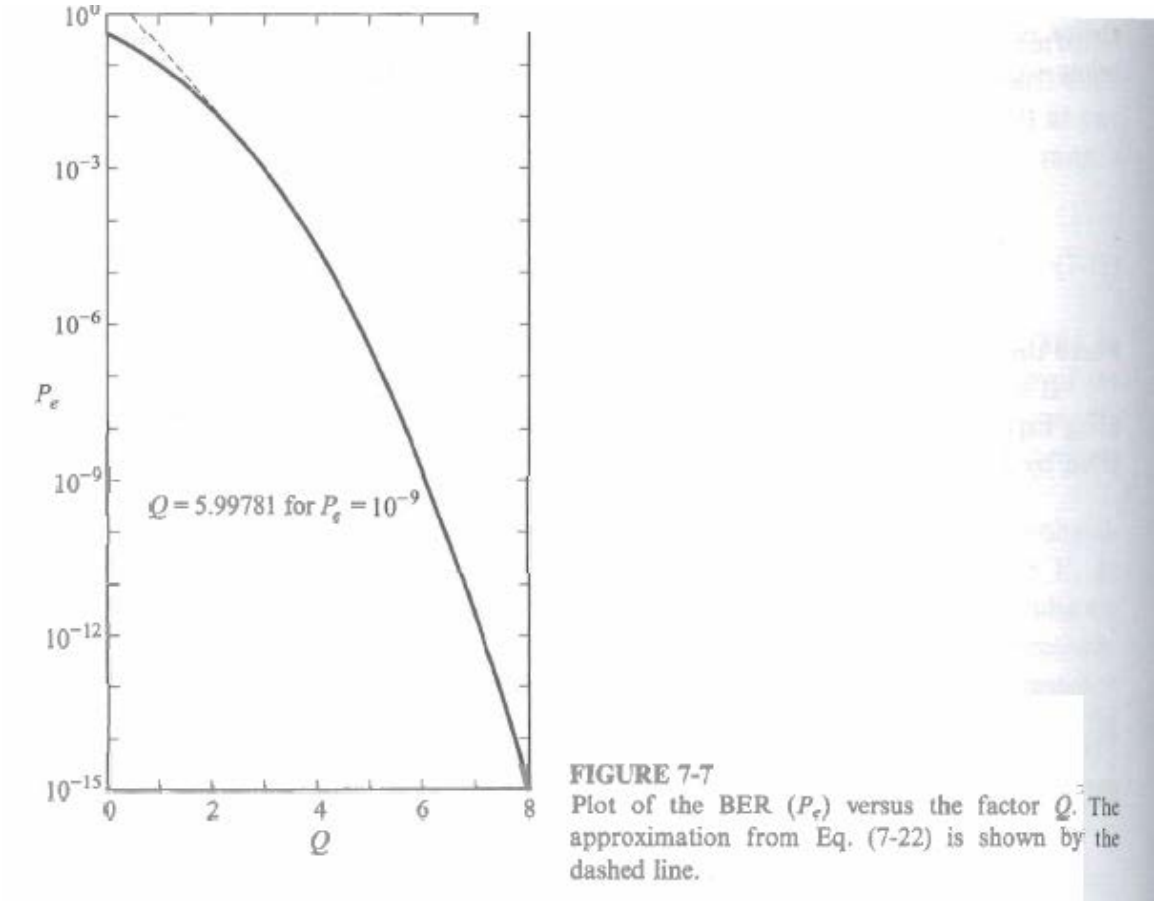

FIGURE 7-7
Plot of the BER (P_e) versus the factor Q. The approximation from Eq. (7-22) is shown by the dashed line.

b. How can we measure the performance fidelity for an analog receiver in terms S/N ratio? (8)

Answer:

7.5 ANALOG RECEIVERS

In addition to the wide usage of fiber optics for the transmission of digital signals, there are many potential applications for analog links. These range from individual 4-kHz voice channels to microwave links operating in the multigigahertz region.[38-40] In the previous sections we discussed digital receiver performance in terms of error probability. For an analog receiver, the performance fidelity is measured in terms of a *signal-to-noise ratio*. This is defined as the ratio of the mean-square signal current to the mean-square noise current.

The simplest analog technique is to use amplitude modulation of the source.[2] In this scheme, the time-varying electric signal $s(t)$ is used to modulate directly an optical source about some bias point defined by the bias current I_B, as shown in Fig. 7-20. The transmitted optical power $P(t)$ is thus of the form

$$P(t) = P_t[1 + ms(t)] \tag{7-100}$$

where P_t is the average transmitted optical power, $s(t)$ is the analog modulation signal, and m is the modulation index defined by (see Sec. 4.4)

$$m = \frac{\Delta I}{I_B} \tag{7-101}$$

Here, ΔI is the variation in current about the bias point. In order not to introduce distortion into the optical signal, the modulation must be confined to the linear

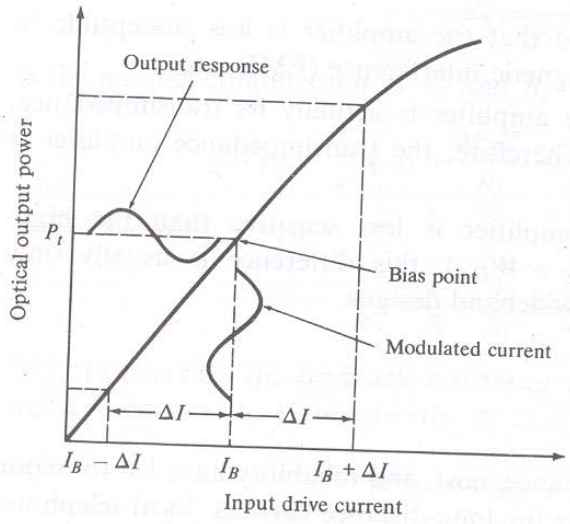

FIGURE 7-20
Direct analog modulation of an LED source.

region of the light source output curve shown in Fig. 7-20. Also, if $\Delta I > I_B$, the lower portion of the signal gets cut off and severe distortion results.

At the receiver end, the photocurrent generated by the analog optical signal is

$$\begin{aligned} i_s(t) &= \mathscr{R}_0 M P_r[1 + ms(t)] \\ &= I_p M[1 + ms(t)] \end{aligned} \tag{7-102}$$

where $\mathscr{R}_0$ is the detector responsivitity, P_r is the average received optical power, $I_p = \mathscr{R}_0 P_r$ is the primary photocurrent, and M is the photodetector gain. If $s(t)$ is a sinusoidally modulated signal, then the mean-square signal current at the photodetector output is (ignoring a dc term)

$$\langle i_s^2 \rangle = \tfrac{1}{2}(\mathscr{R}_0 M m P_r)^2 = \tfrac{1}{2}(M m I_p)^2 \tag{7-103}$$

Recalling from Eq. (6-18) that the mean-square noise current for a photodiode receiver is the sum of the mean-square quantum noise current, the equivalent-resistance thermal noise current, the dark noise current, and the surface-leakage noise current, we have

$$\langle i_N^2 \rangle = 2q(I_p + I_D)M^2 F(M) B + 2q I_L B + \frac{4k_B T B}{R} F_t \tag{7-104}$$

where I_p = primary (unmultiplied) photocurrent $= \mathscr{R}_0 P_r$
I_D = primary bulk dark current
I_L = surface-leakage current
$F(M)$ = excess photodiode noise factor $\simeq M^x (0 < x \leq 1)$
B = effective noise bandwidth
R_{eq} = equivalent resistance of photodetector load and amplifier
F_t = noise figure of the baseband amplifier

By a suitable choice of the photodetector, the leakage current can be rendered negligible. With this assumption, the signal-to-noise ratio S/N is

$$\begin{aligned} \frac{S}{N} = \frac{\langle i_s^2 \rangle}{\langle i_N^2 \rangle} &= \frac{\tfrac{1}{2}(\mathscr{R}_0 M m P_r)^2}{2q(\mathscr{R}_0 P_r + I_D)M^2 F(M) B + (4k_B T B / R_{eq}) F_t} \\ &= \frac{\tfrac{1}{2}(I_p M m)^2}{2q(I_p + I_D)M^2 F(M) B + (4k_B T B / R_{eq}) F_t} \end{aligned} \tag{7-105}$$

For a *pin* photodiode we have $M = 1$. When the optical power incident on the photodiode is small, the circuit noise term dominates the noise current, so that

$$\frac{S}{N} \simeq \frac{\tfrac{1}{2} m^2 I_p^2}{(4k_B T B / R_{eq}) F_t} = \frac{\tfrac{1}{2} m^2 \mathscr{R}_0^2 P_r^2}{(4k_B T B / R_{eq}) F_t} \tag{7-106}$$

Here, the signal-to-noise ratio is directly proportional to the square of the photodiode output current and inversely proportional to the thermal noise of the circuit.

For large optical signals incident on a *pin* photodiode, the quantum noise associated with the signal detection process dominates, so that

$$\frac{S}{N} \simeq \frac{m^2 I_p}{4qB} = \frac{m^2 \mathcal{R}_0 P_r}{4qB} \tag{7-107}$$

Since the signal-to-noise ratio in this case is independent of the circuit noise, it represents the fundamental or quantum limit for analog receiver sensitivity.

When an avalanche photodiode is employed at low signal levels and with low values of gain M, the circuit noise term dominates. At a fixed low signal level, as the gain is increased from a low value, the signal-to-noise ratio increases with gain until the quantum noise term becomes comparable to the circuit noise term. As the gain is increased further beyond this point, the signal-to-noise ratio *decreases* as $F(M)^{-1}$. Thus, for a given set of operating conditions, there exists an optimum value of the avalanche gain for which the signal-to-noise ratio is a maximum. Since an avalanche photodiode increases the signal-to-noise ratio for small optical signal levels, it is the preferred photodetector for this situation.

For very large optical signal levels, the quantum noise term dominates the receiver noise. In this case, an avalanche photodiode serves no advantage, since the detector noise increases more rapidly with increasing gain M than the signal level. This is shown in Fig. 7-21, where we compare the signal-to-noise ratio for a *pin* and an avalanche photodiode receiver as a function of the received optical power. The signal-to-noise ratio for the avalanche photodetector is at the optimum gain (see Probs. 7-28 and 7-29). The parameter values chosen for this

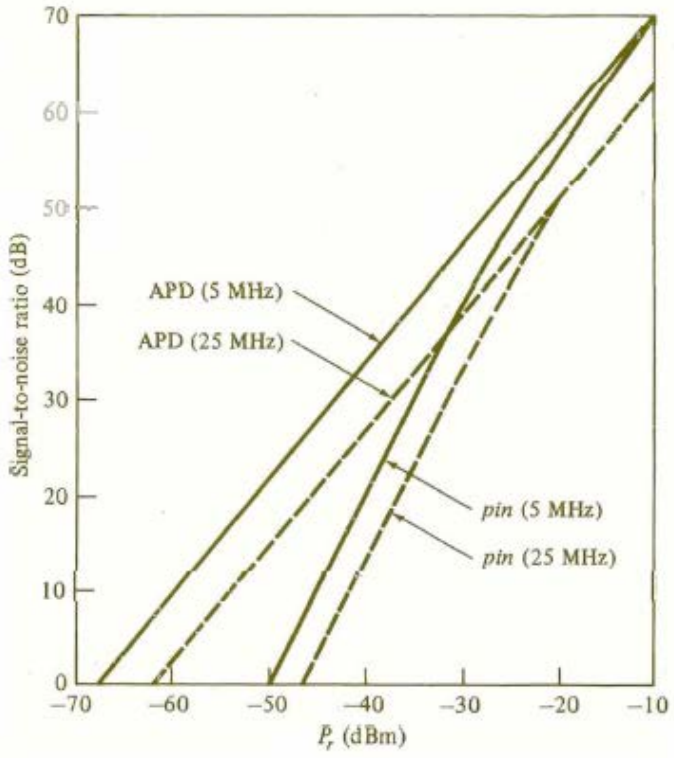

FIGURE 7-21
Comparison of the signal-to-noise ratio for *pin* and avalanche photodiodes as a function of received optical power for bandwidths of 5 and 25 MHz.

example are $B = 5$ MHz and 25 MHz, $x = 0.5$ for the avalanche photodiode and 0 for the *pin* diode, $m = 80$ percent, $\mathcal{R}_0 = 0.5$ A/W, and $R_{eq}/F_t = 10^4\ \Omega$. We see that for low signal levels an avalanche photodiode yields a higher signal-to-noise ratio, whereas at large received optical power levels a *pin* photodiode gives better performance.

Q.7 a. Explain the implementation of an Analog Fibre Optic System. How will you analyse the performance of analog system through CNR? (8)

Answer:

9.1 OVERVIEW OF ANALOG LINKS

Figure 9-1 shows the basic elements of an analog link. The transmitter contains either an LED or a laser diode optical source. As noted in Sec. 4.4 and shown in Fig. 4-35, in analog applications, one first sets a bias point on the source approximately at the midpoint of the linear output region. The analog signal can then be sent using one of several modulation techniques. The simplest form for optical fiber links is direct intensity modulation, wherein the optical output from the source is modulated simply by varying the current around the bias point in proportion to the message signal level. Thus, the information signal is transmitted directly in the baseband.

A somewhat more complex but often more efficient method is to translate the baseband signal onto an electrical subcarrier prior to intensity modulation of the source. This is done using standard amplitude-modulation (AM), frequency-modulation (FM), or phase-modulation (PM) techniques.[10,11] No matter which method is implemented, one must pay careful attention to signal impairments in the optical source. These include harmonic distortions, intermodulation products, relative intensity noise (RIN) in the laser, and laser clipping.[12]

In relation to the fiber-optic element shown in Fig. 9-1, one must take into account the frequency dependence of the amplitude, phase, and group delay in the fiber. Thus, the fiber should have a flat amplitude and group-delay response within the passband required to send the signal free of linear distortion. In addition, since modal-distortion-limited bandwidth is difficult to equalize, it is best to choose a single-mode fiber. The fiber attenuation is also important, since the carrier-to-noise performance of the system will change as a function of the received optical power.

The use of an optical amplifier in the link leads to additional noise, known as amplified spontaneous emission (ASE), as is described in Chap. 11. In the

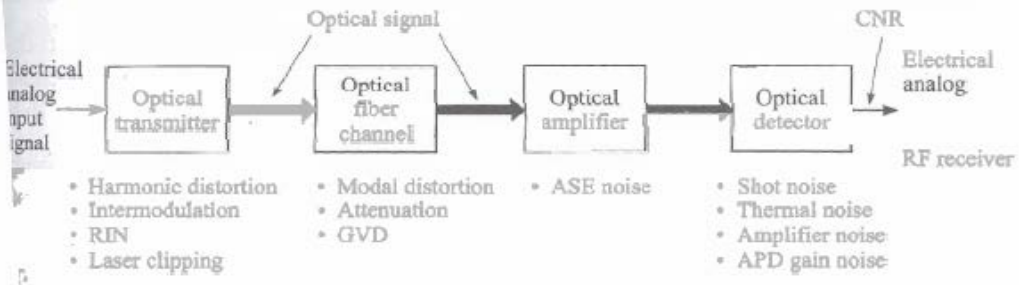

URE 9-1
ic elements of an analog link and the major noise contributors.

optical receiver, the principal impairments are quantum or shot noise, APD gain noise, and thermal noise.

9.2 CARRIER-TO-NOISE RATIO

In analyzing the performance of analog systems, one usually calculates the ratio of rms carrier power to rms noise power at the input of the RF receiver following the photodetection process. This is known as the *carrier-to-noise ratio* (CNR). Let us look at some typical CNR values for digital and analog data. For digital data, consider the use of frequency-shift keying (FSK). In this modulation scheme, the amplitude of a sinusoidal carrier remains constant, but the phase shifts from one frequency to another to represent binary signals. For FSK, BERs of 10^{-9} and 10^{-15} translate into CNR values of 36 (15.6 dB) and 64 (18.0 dB), respectively. The analysis for analog signals is more complex, since it sometimes depends on user perception of the signal quality, such as in viewing a television picture. A widely used analog signal is a 525-line studio-quality television signal. Using amplitude modulation (AM) for such a signal requires a CNR of 56 dB, since the need for bandwidth efficiency leads to a high signal-to-noise ratio. Frequency modulation (FM), on the other hand, only needs CNR values of 15–18 dB.

If CNR_i represents the carrier-to-noise ratio related to a particular signal contaminant (e.g., shot noise), then for N signal-impairment factors the total CNR is given by

$$\frac{1}{\text{CNR}} = \sum_{i=1}^{N} \frac{1}{\text{CNR}_i} \tag{9-1}$$

For links in which only a single information channel is transmitted, the important signal impairments include laser intensity noise fluctuations, laser clipping, photodetector noise, and optical-amplifier noise. When multiple message channels operating at different carrier frequencies are sent simultaneously over the same fiber, then harmonic and intermodulation distortions arise. Furthermore, the inclusion of an optical amplifier gives rise to ASE noise. In principle, the three dominant factors that cause signal impairments in a fiber link are shot noise, optical-amplifier noise, and laser clipping.[12] Most other degradation effects can be sufficiently reduced or eliminated.

In this section, we shall first examine a simple single-channel amplitude-modulated signal sent at baseband frequencies. Section 9.3 addresses multichannel systems in which intermodulation noise becomes important. Problem 9-10 gives expressions for the effects of laser clipping and ASE noise.

b. Explain the following: (8)
(i) Multichannel Amplitude Modulation
(ii) Subcarrier Multiplexing

Answer:

9.3.1 Multichannel Amplitude Modulation

The initial widespread application of analog fiber optic links, which started in the late 1980s, was to CATV networks.[14-17] These coax-based television networks operate in a frequency range from 50 to 88 MHz and from 120 to 550 MHz. The band from 88 to 120 MHz is not used, since it is reserved for FM radio broadcast. The CATV networks can deliver over 80 amplitude-modulated vestigial-sideband (AM-VSB) video channels, each having a noise bandwidth of 4 MHz within a channel bandwidth of 6 MHz, with signal-to-noise ratios exceeding 47 dB. To remain compatible with existing coax-based networks, a multichannel AM-VSB format was also chosen for the fiber optic system.

Figure 9-7 depicts the technique for combining N independent messages. An information-bearing signal on channel i amplitude-modulates a carrier wave that has a frequency f_i, where $i = 1, 2 \ldots, N$. An RF power combiner then sums these N amplitude-modulated carriers to yield a composite frequency-division-multiplexed (FDM) signal which intensity-modulates a laser diode. Following the optical receiver, a bank of parallel bandpass filters separates the combined carriers back into individual channels. The individual message signals are recovered from the carriers by standard RF techniques.

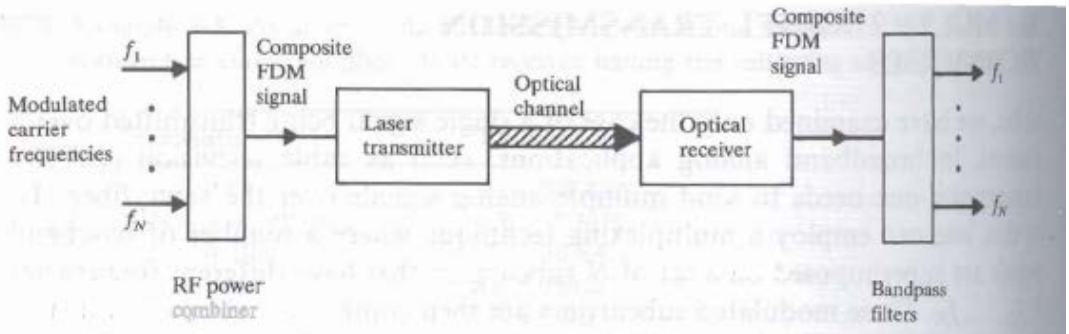

FIGURE 9-7
Standard technique for frequency-division multiplexing of N independent information-bearing signals.

For a large number of FDM carriers with random phases, the carriers add on a power basis. Thus, for N channels the optical modulation index m is related to the per-channel modulation index m_i by

$$m = \left(\sum_{i=1}^{N} m_i^2 \right)^{1/2} \tag{9-14a}$$

If each channel modulation index m_i has the same value m_c, then

$$m = m_c N^{0.5} \tag{9-14b}$$

As a result, when N signals are frequency-multiplexed and used to modulate a single optical source, the carrier-to-noise ratio of a single channel is degraded by $10 \log N$. If only a few channels are combined, the signals will add in voltage rather than power, so that the degradation will have a $20 \log N$ characteristic.

When multiple carrier frequencies pass through a nonlinear device such as a laser diode, signal products other than the original frequencies can be produced. As noted in Sec. 4.4, these undesirable signals are called *intermodulation products* and they can cause serious interference in both in-band and out-of-band channels. The result is a degradation of the transmitted signal. Among the intermodulation products, generally only the second-order and third-order terms are considered, since higher-order products tend to be significantly smaller.

Third-order intermodulaton (IM) distortion products at frequencies $f_i + f_j - f_k$ (which are known as *triple-beat IM products*) and $2f_i - f_j$ (which are known as *two-tone third-order IM products*) are the most dominant, since many of these fall within the bandwidth of a multichannel system. For example, a 50-channel CATV network operating over a standard frequency range of 55.25–373.25 MHz has 39 second-order IM products at 54.0 MHz and 786 third-order IM tones at 229.25 MHz. The amplitudes of the triple-beat products are 3 dB higher than the two-tone third-order IM products. In addition, since there are $N(N-1)(N-2)/2$ triple-beat terms compared with $N(N-1)$ two-tone third-order terms, the triple-beat products tend to be the major source of IM noise.

If a signal passband contains a large number of equally spaced carriers, several IM terms will exist at or near the same frequency. This so-called *beat*

TABLE 9-1
Distribution of the number of third-order triple-beat intermodulation products for the number of channels N ranging from 1 to 8

	r							
N	1	2	3	4	5	6	7	8
1	0							
2	0	0						
3	0	1	0					
4	1	2	2	1				
5	2	4	4	4	2			
6	4	6	7	7	6	4		
7	6	9	10	11	10	9	6	
8	9	12	14	15	15	14	12	9

stacking is additive on a power basis. For example, for N equally spaced equal-amplitude carriers, the number of third-order IM products that fall right on the rth carrier is given by[18,19]

$$D_{1,2} = \tfrac{1}{2}\{N - 2 - \tfrac{1}{2}[1 - (-1)^N](-1)^r\} \tag{9-15}$$

for two-tone terms of the type $2f_i - f_j$, and by

$$D_{1,1,1} = \frac{r}{2}(N - r + 1) + \tfrac{1}{4}\{(N-3)^2 - 5 - \tfrac{1}{2}[1 - (-1)^N](-1)^{N+r}\} \tag{9-16}$$

for triple-beat terms of the type $f_i + f_j - f_k$.

Whereas the two-tone third-order terms are fairly evenly spread through the operating passband, the triple-beat products tend to be concentrated in the middle of the channel passband, so that the center carriers receive the most intermodulation interference. Tables 9-1 and 9-2 show the distributions of the *third-order* triple-beat and *two-tone IM* products for the number of channels N ranging from 1 to 8.

TABLE 9-2
Distribution of the number of third-order two-tone intermodulation products for the number of channels N ranging from 1 to 8

	r							
N	1	2	3	4	5	6	7	8
1	0							
2	0	0						
3	1	0	1					
4	1	1	1	1				
5	2	1	2	1	2			
6	2	2	2	2	2	2		
7	3	2	3	2	3	2	3	
8	3	3	3	3	3	3	3	3

The results of beat stacking are commonly referred to as *composite second order (CSO)* and *composite triple beat (CTB)*, and are used to describe the performance of multichannel AM links. These are defined as[20]

$$\text{CSO} = \frac{\text{peak carrier power}}{\text{peak power in composite 2nd-order IM tone}} \tag{9-17}$$

and

$$\text{CTB} = \frac{\text{peak carrier power}}{\text{peak power in composite 3rd-order IM tone}} \tag{9-18}$$

9.3.3 Subcarrier Multiplexing

There is also great interest in using RF or *microwave subcarrier multiplexing* for high-capacity lightwave systems.[1,25–28] The term *subcarrier multiplexing* (SCM) is used to describe the capability of multiplexing both multichannel analog and digital signals within the same system.

Figure 9-12 shows the basic concept of an SCM system. The input to the transmitter consists of a mixture of N independent analog and digital baseband signals. These signals can carry either voice, data, video, digital audio, high-definition video, or any other analog or digital information. Each incoming signal $s_i(t)$ is mixed with a local oscillator (LO) having a frequency f_i. The local oscillator frequencies employed are in the 2-to-8-GHz range and are known as the *subcarriers*. Combining the modulated subcarriers gives a composite frequency-division-multiplexed signal which is used to drive a laser diode.

At the receiving end, the optical signal is directly detected with a high-speed wideband InGaAs *pin* photodiode and reconverted to a microwave signal. For long-distance links, one can also employ a wideband InGaAs avalanche photodiode with a 50- to 80-GHz gain–bandwidth product or use an optical preamplifier. For amplifying the received microwave signal, one can use a commercially available wideband low-noise amplifier or a *pin*-FET receiver.

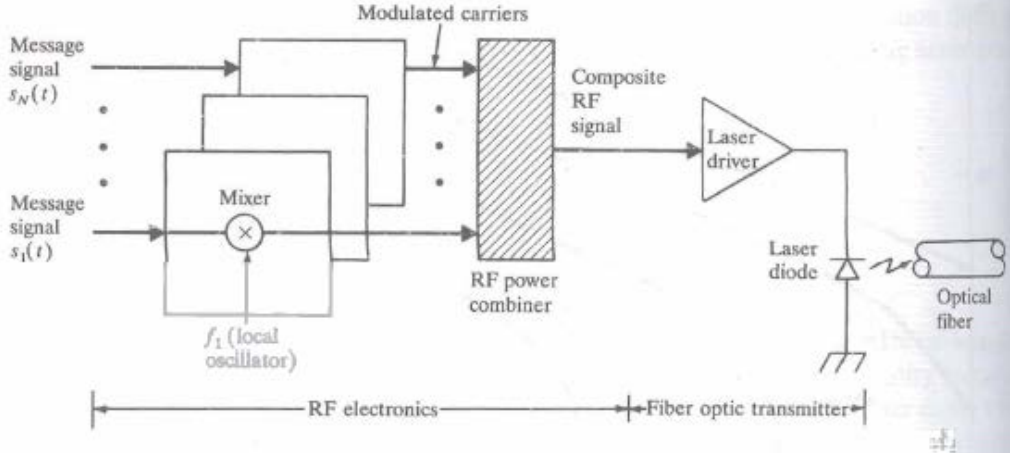

FIGURE 9-12
Basic concept of subcarrier multiplexing. One can simultaneously send analog and digital signals by frequency-division multiplexing them on different subcarrier frequencies.

Q.8 a. Explain the following terms in context with Point - to - Point Links for Digital Transmission:
(i) Link Power Budget
(ii) Rise Time Budget
(iii) Short Wavelength Band (8)

Answer:

8.1.2 Link Power Budget

An optical power loss model for a point-to-point link is shown in Fig. 8-2. The optical power received at the photodetector depends on the amount of light coupled into the fiber and the losses occurring in the fiber and at the connectors and splices. The link loss budget is derived from the sequential loss contributions of each element in the link. Each of these loss elements is expressed in decibels (dB) as

$$\text{loss} = 10 \log \frac{P_{\text{out}}}{P_{\text{in}}} \tag{8-1}$$

where P_{in} and P_{out} are the optical powers emanating into and out of the loss element, respectively.

In addition to the link loss contributors shown in Fig. 8-2, a link power margin is normally provided in the analysis to allow for component aging, temperature fluctuations, and losses arising from components that might be added at future dates. A link margin of 6–8 dB is generally used for systems that are not expected to have additional components incorporated into the link in the future.

The link loss budget simply considers the total optical power loss P_T that is allowed between the light source and the photodetector, and allocates this loss to cable attenuation, connector loss, splice loss, and system margin. Thus, if P_S is the optical power emerging from the end of a fiber flylead attached to the light source, and if P_R is the receiver sensitivity, then

$$\begin{aligned} P_T &= P_S - P_R \\ &= 2l_c + \alpha_f L + \text{system margin} \end{aligned} \tag{8-2}$$

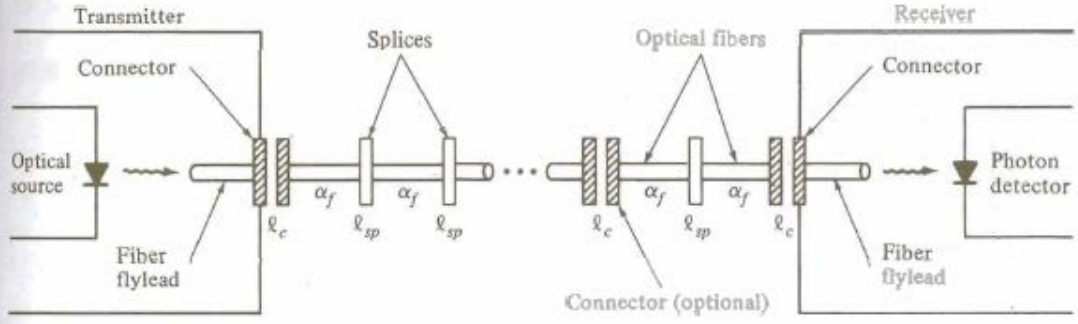

FIGURE 8-2
Optical power loss model for a point-to-point link. The losses occur at connectors (l_c), at splices (l_{sp}), and in the fiber (α_f).

Here, l_c is the connector loss, α_f is the fiber attenuation (dB/km), L is the transmission distance, and the system margin is nominally taken as 6 dB. Here, we assume that the cable of length L has connectors only on the ends and none in between. The splice loss is incorporated into the cable loss for simplicity.

8.1.3 Rise-Time Budget

A rise-time budget analysis is a convenient method for determining the dispersion limitation of an optical fiber link. This is particularly useful for digital systems. In this approach, the total rise time t_{sys} of the link is the root sum square of the rise times from each contributor t_i to the pulse rise-time degradation:

$$t_{sys} = \left(\sum_{i=1}^{N} t_i^2 \right)^{1/2} \tag{8-3}$$

The four basic elements that may significantly limit system speed are the transmitter rise time t_{tx}, the group-velocity dispersion (GVD) rise time t_{GVD} of the fiber, the modal dispersion rise time t_{mod} of the fiber, and the receiver rise time t_{rx}. Single-mode fibers do not experience modal dispersion, so in these fibers the rise time is related only to GVD. Generally, the total transition-time degradation of a digital link should not exceed 70 percent of an NRZ (non-return-to-zero) bit period or 35 percent of a bit period for RZ (return-to-zero) data, where one bit period is defined as the reciprocal of the data rate (NRZ and RZ data formats are discussed in more detail in Sec. 8.2).

The rise times of transmitters and receivers are generally known to the designer. The transmitter rise time is attributable primarily to the light source and its drive circuitry. The receiver rise time results from the photodetector response and the 3-dB electrical bandwidth of the receiver front end. The response of the receiver front end can be modeled by a first-order lowpass filter having a step response[9]

$$g(t) = [1 - \exp(-2\pi B_{rx} t)]u(t)$$

where B_{rx} is the 3-dB electrical bandwidth of the receiver and $u(t)$ is the unit step function which is 1 for $t \geq 0$ and 0 for $t < 0$. The rise time t_{rx} of the receiver is usually defined as the time interval between $g(t) = 0.1$ and $g(t) = 0.9$. This is known as the *10- to 90-percent rise time*. Thus, if B_{rx} is given in megahertz, then the receiver front-end rise time in nanoseconds is (see Prob. 8-3)

$$t_{rx} = \frac{350}{B_{rx}} \tag{8-4}$$

In practice, an optical fiber link seldom consists of a uniform, continuous, jointless fiber. Instead, a transmission link nominally is formed from several concatenated (tandemly joined) fibers that may have different dispersion characteristics. This is especially true for dispersion-compensated links operating at 10 Gb/s and higher (see Chap. 12). In addition, multimode fibers experience modal distributions at fiber-to-fiber joints owing to misaligned joints, different core index profiles in each fiber, and/or different degrees of mode mixing in individual fibers. Determining the fiber rise times resulting from GVD and modal dispersion then becomes more complex than for the case of a single uniform fiber.

The fiber rise time t_{GVD} resulting from GVD over a length L can be approximated by Eq. (3-54) as

$$t_{GVD} \approx |D| L \sigma_\lambda \tag{8-5}$$

where σ_λ is the half-power spectral width of the source, and the dispersion D is given by Eq. (3-57) for a non-dispersion-shifted fiber and by Eq. (3-59) for a dispersion-shifted fiber. Since the dispersion value generally changes from fiber section to section in a long link, an average value should be used for D in Eq. (8-5).

The difficulty in predicting the bandwidth (and hence the modal rise time) of a series of concatenated multimode fibers arises from the observation that the total route bandwidth can be a function of the order in which fibers are joined. For example, instead of randomly joining together arbitrary (but very similar) fibers, an improved total link bandwidth can be obtained by selecting adjoining fibers with alternating over- and undercompensated refractive-index profiles to provide some modal delay equalization. Although the ultimate concatenated fiber bandwidth can be obtained by judiciously selecting adjoining fibers for optimum modal delay equalization, in practice this is unwieldy and time-consuming, particularly since the initial fiber in the link appears to control the final link characteristics.

A variety of empirical expressions for modal dispersion have thus been developed.[10-15] From practical field experience, it has been found that the bandwidth B_M in a link of length L can be expressed to a reasonable approximation by the empirical relation

$$B_M(L) = \frac{B_0}{L^q} \tag{8-6}$$

where the parameter q ranges between 0.5 and 1, and B_0 is the bandwidth of a 1-km length of cable. A value of $q = 0.5$ indicates that a steady-state modal equilibrium has been reached, whereas $q = 1$ indicates little mode mixing. Based on field experience, a reasonable estimate is $q = 0.7$.

Another expression that has been proposed for B_M, based on curve fitting of experimental data, is

$$\frac{1}{B_M} = \left[\sum_{n=1}^{N}\left(\frac{1}{B_n}\right)^{1/q}\right]^{q} \tag{8-7}$$

where the parameter q ranges between 0.5 (quadrature addition) and 1.0 (linear addition), and B_n is the bandwidth of the nth fiber section. Alternatively, Eq. (8-7) can be written as

$$t_M(N) = \left[\sum_{n=1}^{N}(t_n)^{1/q}\right]^{1} \tag{8-8}$$

where $t_M(N)$ is the pulse broadening occurring over N cable sections in which the individual pulse broadenings are given by t_n.

We now need to find the relation between the fiber rise time and the 3-dB bandwidth. For this, we use a variation of the expression derived by Midwinter.[16] We assume that the optical power emerging from the fiber has a gaussian temporal response described by

$$g(t) = \frac{1}{\sqrt{2\pi}\sigma}e^{-t^2/2\sigma^2} \tag{8-9}$$

where σ is

The Fourier transform of this function is

$$G(\omega) = \frac{1}{\sqrt{2\pi}}e^{-\omega^2\sigma^2/2} \tag{8-10}$$

From Eq. (8-9) the time $t_{1/2}$ required for the pulse to reach its half-maximum value; that is, the time required to have

$$g(t_{1/2}) = 0.5g(0) \tag{8-11}$$

is given by

$$t_{1/2} = (2\ln 2)^{1/2}\sigma \tag{8-12}$$

If we define the time t_{FWHM} as the full width of the pulse at its half-maximum value, then

$$t_{\mathrm{FWHM}} = 2t_{1/2} = 2\sigma(2\ln 2)^{1/2} \tag{8-13}$$

The 3-dB optical bandwidth $B_{3\mathrm{dB}}$ is defined as the modulation frequency $f_{3\mathrm{dB}}$ at which the received optical power has fallen to 0.5 of the zero frequency value. Thus, from Eqs. (8-10) and (8-13), we find that the relation between the full-width half-maximum rise time t_{FWHM} and the 3-dB optical bandwidth is

$$f_{3dB} = B_{3dB} = \frac{0.44}{t_{FWHM}} \tag{8-14}$$

Using Eq. (8-6) for the 3-dB optical bandwidth of the fiber link and letting t_{FWHM} be the rise time resulting from modal dispersion, then, from Eq. (8-14),

$$t_{mod} = \frac{0.44}{B_M} = \frac{0.44L^q}{B_0} \tag{8-15}$$

If t_{mod} is expressed in nanoseconds and B_M is given in megahertz, then

$$t_{mod} = \frac{440}{B_M} = \frac{440L^q}{B_0} \tag{8-16}$$

Substituting Eqs. (3-20), (8-4), and (8-16) into Eq. (8-3) gives a total system rise time of

$$t_{sys} = \left[t_{tx}^2 + t_{mod}^2 + t_{GVD}^2 + t_{rx}^2\right]^{1/2}$$

$$= \left[t_{tx}^2 + \left(\frac{440L^q}{B_0}\right)^2 + D^2\sigma_\lambda^2 L^2 + \left(\frac{350}{B_{rx}}\right)^2\right]^{1/2} \tag{8-17}$$

where all the times are given in nanoseconds, σ_λ is the half-power spectral width of the source, and the dispersion D [expressed in ns/(nm · km)] is given by Eq. (3-57) for a non-dispersion-shifted fiber and by Eq. (3-59) for a dispersion-shifted fiber. In the 800-to-900-nm region, D is about 0.07 ns/(nm · km), which is principally due to material dispersion, so that $t_{GVD}^2 \approx t_{mat}^2 = D_{mat}^2\sigma_\lambda^2 L^2$. Much smaller values of D are seen in the 1300- and 1550-nm window (see Fig. 3-26).

b. What do you understand by error correction & detection in optical fibre communication? Enlist all the techniques employed for correction & detection purpose. Explain one for each. (8)

Answer:

8.3 ERROR CORRECTION

For high-speed broadband networks, the data-transmission reliability provided

is case, the transport protocol of the network must compensate for the differ-
ce in the bit-loss rate. The two basic schemes for improving the reliability are
omatic repeat request (ARQ) and forward error correction (FEC).[39-44] The
) schemes have been used for many years and are widely implemented. As
in Fig. 8-10, the technique uses a feedback channel between the receiver
transmitter to request message retransmission in case errors are detected
eiver. Since each such retransmission adds at least one roundtrip time of
RQ may not be feasible for applications that require low latency.
se applications are voice and video services that involve human inter-
ess control, and remote sensing in which data must arrive within a
in order to be useful.

FIGURE 8-10
Basic setup for an automatic-repeat-request (ARQ) error-correction scheme.

Forward error correction avoids the shortcomings of ARQ for high bandwidth optical networks that require low delays. In FEC techniques, redundant information is transmitted along with the original information. If some of the original data is lost or received in error, the redundant information is used to reconstruct it. Typically, the amount of redundant information is small, so the FEC scheme does not use up much additional bandwidth and thus remains efficient. Depending on the application, some considerations of FEC code properties include the ability to accommodate self-synchronous scramblers (with characteristics polynomial $1 + x^{43}$) used in SONET (see Chap. 12), the 4B5B line code used in FDDI, or the 8B10B line code used in Fibre Channel.

The most popular error-correction codes are *cyclic codes*. These are designated by the notation (n, m), where n equals the number of original bits m plus the number of redundant bits. Some examples that have been used include a (224, 216) shortened Hamming code,[40] a (192, 190) Reed-Solomon code,[42] a (255, 239) Reed-Solomon code,[43] and (18880, 18865) and (2370, 2358) shortened Hamming

The results of the (224, 216) code are shown in Figs. 8-11 and 8-12. Figure 8-11 is a plot of the FEC-decoded BER versus the primary BER. The data is from an experiment using a 565-Mb/s multimode laser system operating at 1300 nm. The laser had a FWHM of 4 nm at the one-tenth-maximum point. Various levels of AWGN (additive white gaussian noise) were injected at the receiver decision point in order to vary the signal-to-noise ratio. The relative performance improvement using FEC increases as the error probability decreases. For example, at a 10^{-4} primary BER the performance improves by a factor of about 25, whereas at a 10^{-6} primary error level the BER resulting from FEC decreases by a factor of about 3000.

Figure 8-12 shows the measured BER performance as a function of the received power level with and without FEC. Analogous to Fig. 8-11, the performance improvement with FEC is significant.

Q.9 a. Define WDM? With the help of schematic, explain the operational principles of WDM. (8)

Answer:

A powerful aspect of an optical communication link is that many different wavelengths can be sent along a single fiber simultaneously in the 1300-to-1600-nm spectral band. The technology of combining a number of wavelengths onto the same fiber is known as *wavelength-division multiplexing* or WDM.[1-7] Conceptually, the WDM scheme is the same as frequency-division multiplexing (FDM) used in microwave radio and satellite systems. Just as in FDM, the wavelengths (or optical frequencies) in WDM must be properly spaced to avoid interchannel interference. The key system features of WDM are as follows:

10.1 OPERATIONAL PRINCIPLES OF WDM

In standard point-to-point links a single fiber line has one optical source at its transmitting end and one photodetector at the receiving end. Signals from different light sources use separate and uniquely assigned optical fibers. Since an optical source has a narrow linewidth, this type of transmission makes use of only a very narrow portion of the transmission bandwidth capability of a fiber.

To see the potential of WDM, let us first examine the characteristics of a high-quality optical source. As an example, the modulated output of a DFB laser has a frequency spectrum of 10–50 MHz, which is equivalent to a nominal spectral linewidth of 10^{-3} nm. When using such a source, a guard band of 0.4–1.6 nm is typically employed. This is done to take into account possible drifts of the peak wavelength due to aging or temperature effects, and to give both the manufacturer and the user some leeway in specifying and choosing the precise peak emission wavelength. With such spectral bandwidths, simplex systems make use of only a small portion of the transmission bandwidth capability of a standard fiber. This can be seen from Fig. 10-1, which depicts the attenuation of light in a silica fiber as a function of wavelength. The curve shows that the two low-loss regions of a single-mode fiber extend over the wavelengths ranging from about 1270 to 1350 nm (the 1310-nm window) and from 1480 to 1600 nm (the 1550-nm window). However, note the wider window of AllWave® fibers in Fig. 3-1.

We can view these regions either in terms of spectral width (the wavelength band occupied by the light signal and its guard band) or by means of optical bandwidth (the frequency band occupied by the light signal). To find the optical bandwidth corresponding to a particular spectral width in these regions, we use

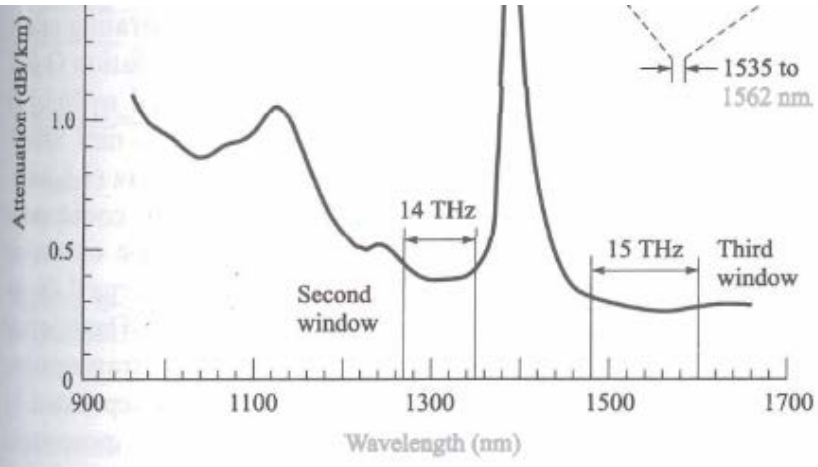

FIGURE 10-1
The transmission bandwidths in the 1310-nm and 1550-nm windows allow the use of many simultaneous channels for sources with narrow spectral widths. The ITU-T standard for WDM specifies channels with 100-GHz spacings. Also, see Fig. 3-1 for water-free AllWave® fiber.

the relationship $c = \lambda\nu$, which relates the wavelength λ to the carrier frequency ν, where c is the speed of light. Differentiating this we have for $\Delta\lambda << \lambda^2$

$$|\Delta\nu| = \left(\frac{c}{\lambda^2}\right)|\Delta\lambda| \qquad (10\text{-}1)$$

where the deviation in frequency $\Delta\nu$ corresponds to the wavelength deviation $\Delta\lambda$ around λ. From Eq. (10-1), the optical bandwidth is $\Delta\nu = 14$ THz for a usable spectral band $\Delta\lambda = 80$ nm in the 1310-nm window. Similarly, $\Delta\nu = 15$ THz for a usable spectral band $\Delta\lambda = 120$ nm in the 1550-nm window. This yields a total available fiber bandwidth of about 30 THz in the two low-loss windows.

Since the spectral width of a high-quality source occupies only a narrow optical bandwidth, the two low-loss windows provide many additional operating regions. By using a number of light sources, each emitting at a different peak wavelength that is sufficiently spaced from its neighbor so as not to create interference, the integrities of the independent messages from each source are maintained for subsequent conversion to electrical signals at the receiving end.

b. Briefly explain the following:- (any <u>TWO</u>)
(i) SOA
(ii) SDH/SONET
(iii) Optical CDMA **(8)**

Answer:

11.2 SEMICONDUCTOR OPTICAL AMPLIFIERS

The two major types of SOAs are the resonant, Fabry-Perot amplifier (FPA) and the nonresonant, traveling-wave amplifier (TWA).[5–8] In an FPA, the two cleaved facets of a semiconductor crystal act as partially reflective end mirrors that form a Fabry-Perot cavity.[9,10] The natural reflectivity of the facets is approximately 32 percent. This is sometimes enhanced by means of a reflective dielectric coating deposited on the ends. When an optical signal enters the FPA, it gets amplified as

it reflects back and forth between the mirrors until it is emitted at a higher intensity. Although FPAs are easy to fabricate, the optical signal gain is very sensitive to variations in amplifier temperature and input optical frequency. Thus, they require very careful stabilization of temperature and injection current.

The structure of a traveling-wave amplifier is the same as that of an FPA except that the end facets are either antireflection-coated or cleaved at an angle, so that internal reflection does not take place. Thus, the input light gets amplified only once during a single pass through the TWA. These devices have been used more widely than FPAs because they have a large optical bandwidth, high saturation power, and low polarization sensitivity. Since the 3-dB bandwidth of TWAs is about three orders of magnitude greater than that of FPAs, TWAs have become the SOA of choice for networking applications. In particular, TWAs are used as amplifiers in the 1300-nm window and as wavelength converters in the 1550-nm region. For most cases, recent literature on optical fiber systems uses the term "SOA," without qualification, for traveling-wave semiconductor optical amplifiers. In this section, we will concentrate on TWAs only.

12.2 SONET/SDH

With the advent of fiber optic transmission lines, the next step in the evolution of the digital time-division-multiplexing (TDM) scheme was a standard signal format called *synchronous optical network (SONET)* in North America and *synchronous digital hierarchy (SDH)* in other parts of the world. This section addresses the basic concepts of SONET/SDH, its optical interfaces, and fundamental network implementations. The aim here is to discuss only the physical-layer aspects of SONET/SDH as they relate to optical transmission lines and optical networks. Topics such as the detailed data format structure, SONET/SDH operating specifications, and the relationships of switching methodologies such as asynchronous transfer mode (ATM) with SONET/SDH are beyond the scope of this text. These can be found in numerous sources, such as those listed in Refs. 13–15.

12.8 OPTICAL CDMA

In long-haul optical fiber transmission links and networks, the information consists of a multiplexed aggregate data stream originating from many individual subscribers and normally is sent in a well-timed synchronous format. The design goal of this TDM process is to make maximum use of the available optical fiber bandwidth for information transmission, since the multiplexed information stream requires very high-capacity links. To increase the capacity even further, WDM techniques that make use of the wide spectral transmission window of optical fibers are employed. As an alternative to these techniques in a local area network (LAN), optical code-division multiple access (CDMA) has been examined.[94–105] This scheme can provide multiple access to a network without using wavelength-sensitive components as in WDM, and without employing very high-speed electronic data-processing devices as are needed in TDM networks. In the simplest configuration, CDMA achieves multiple access by assigning a unique code to each user. To communicate with another node, users imprint their agreed-upon code onto the data. The receiver can then decode the bit stream by locking onto the same code sequence.

The principle of optical CDMA is based on spread-spectrum techniques, which have been widely used in mobile-satellite and digital-cellular communication systems.[106] The concept is to spread the energy of the optical signal over a frequency band that is much wider than the minimum bandwidth required to send the information. For example, a signal that conveys 10^3 b/s may be spread over a 1 MHz bandwidth. This spreading is done by a code that is independent of the signal itself. Thus, an optical encoder is used to map each bit of information into a high-rate (longer code-length) *optical sequence*.

The symbols in the spreading code are called *chips*, and the energy density of the transmitted waveform is distributed more or less uniformly over the entire spread-spectrum bandwidth. The set of optical sequences becomes a set of unique *address codes* or *signature sequences* for the individual network users. In this addressing scheme, each 1 data bit is encoded into a waveform or signature sequence $s(n)$ consisting of N chips, which represents the destination address of that bit. The 0 data bits are not encoded. Ideally, all of the signature sequences would be mutually orthogonal, and each receiver would process only the address signals intended for it. However, in practice, "nearly orthogonal" is the best that has been accomplished. Consequently, there is some amount of cross correlation between the various addresses. Figure 12-45 illustrates the encoding scheme. Here, the signature sequence contains six chips. When the data signal contains a 1 data bit, the six-chip sequence is transmitted; no chips are sent for a 0 data bit.

From a simplistic point of view, this unique address-encoding scheme can be considered analogous to having numerous pairs of people, in the same room, talking simultaneously using different languages. Ideally, each communicating pair will understand only their own language, so that interference generated by other speakers is minimal. Thus, time-domain optical CDMA allows a number of users to access a network simultaneously through the use of a common wave-

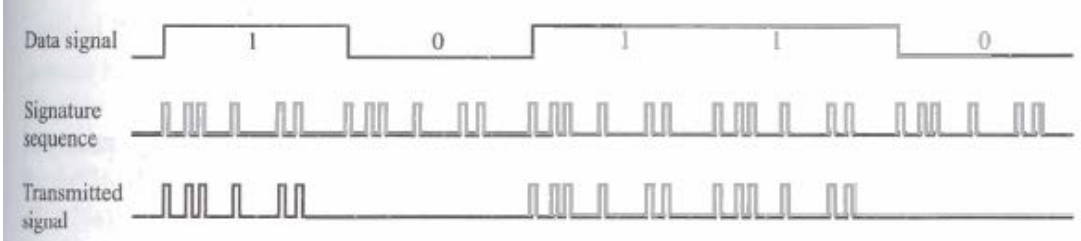

FIGURE 12-45
Example of a six-chip optical CDMA encoding scheme.

length. This is particularly useful in ultrahigh-speed LANs where bit rates of more than 100 Gb/s will be utilized (see Sec. 12.9). A basic limitation of optical CDMA using a coded sequence of pulses is that as the number of users increases, the code length has to be increased in order to maintain the same performance. Since this leads to shorter and shorter pulses, various ideas for mitigating this effect have been proposed. Alternatively, frequency-domain methods based on spectral encoding of broadband incoherent sources (e.g., LEDs or Fabry-Perot lasers) have been proposed.[103,107]

Both asynchronous and synchronous optical CDMA techniques have been examined. Each of these has its strengths and limitations. In general, since synchronous accessing schemes follow rigorous transmission schedules, they produce more successful transmissions (higher throughputs) than asynchronous methods where network access is random and collisions between users can occur. In applications that require real-time transmission, such as voice or interactive video, synchronous accessing techniques are most efficient. When the traffic tends to be bursty in nature or when real-time communication requirements are relaxed, such as in data transmission or file transfers, asynchronous multiplexing schemes are more efficient than synchronous multiplexing.

Figure 12-46 shows an optical CDMA network that is based on the use of a coded sequence of pulses. The setup consists of N transmitter and receiver pairs interconnected in a star network. To send information from node j to node k, the address code for node k is impressed upon the data by the encoder at node j. At the destination, the receiver differentiates between codes by means of correlation detection. That is, each receiver correlates its own address $f(n)$ with the received signal $s(n)$. The receiver output $r(n)$ is

$$r(n) = \sum_{k=1}^{N} s(k) f(k-n) \tag{12-56}$$

If the received signal arrives at the correct destination, then $s(n) = f(n)$, and Eq. (12-56) represents an autocorrelation function. At an incorrect destination, $s(n) \neq f(n)$, and Eq. (12-56) represents a cross-correlation function. For a receiver to be able to distinguish the proper address correctly, it is necessary to maximize the autocorrelation function and minimize the cross-correlation function. This is accomplished by selecting the appropriate code sequence.

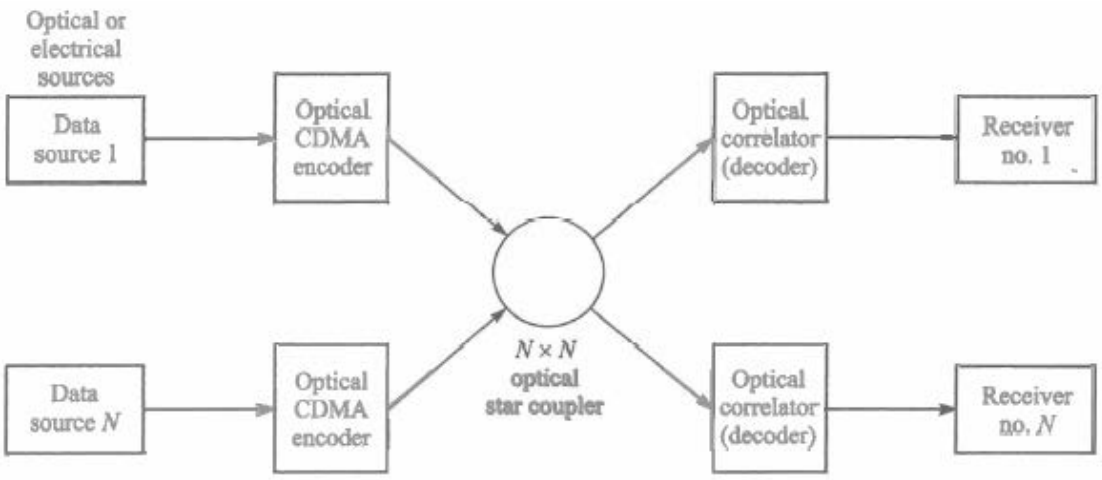

FIGURE 12-46
Example of an optical CDMA network based on using a coded sequence of pulses.

Prime-sequence codes and optical orthogonal codes (OOCs) are the commonly used spreading sequences in optical CDMA systems.[108,109] In addition, bipolar codes have been investigated.[101,110–112] These are particularly suitable for hybrid WDMA/CDMA systems. As noted earlier, some amount of cross correlation exists among the various optical sequences, since the codes devised so far are not perfectly orthogonal. In optical orthogonal codes, for example, there are many more zeros than ones in order to minimize the overlap of different code sequences. If the code words overlap in too many positions, then interference among users will be high. In an OOC system the number of simultaneous users N is bounded by[94]

$$N \leq \left\lfloor \frac{F-1}{K(K-1)} \right\rfloor \tag{12-57}$$

where F is the length of the code sequence and K is the *weight* or the number of ones in the sequence. Here, the symbol $\lfloor x \rfloor$ denotes the integer portion of the real value of x.

TEXT BOOK

I. Optical Fiber Communications, Gerd Keiser, 3rd Edition, McGraw Hill Publications, 2000